

UNIVERSITÉ DU QUÉBEC À MONTRÉAL

MODELING THE SPATIAL AND TEMPORAL VARIABILITY OF DISSOLVED
CO₂ AND CH₄ CONCENTRATIONS OF THE LA ROMAINE HYDROPOWER
COMPLEX

MÉMOIRE
PRÉSENTÉ
COMME EXIGENCE PARTIELLE
DE LA MAÎTRISE EN BIOLOGIE

PAR
FELIPE RUST DE CARVALHO

MAI 2021

UNIVERSITÉ DU QUÉBEC À MONTRÉAL

MODÉLISATION DE LA VARIABILITÉ SPATIALE ET TEMPORELLE DES
CONCENTRATIONS DE CO₂ ET DE CH₄ DISSOUS DU COMPLEXE
HYDROÉLECTRIQUE DE LA ROMAINE

MÉMOIRE
PRÉSENTÉ
COMME EXIGENCE PARTIELLE
DE LA MAÎTRISE EN BIOLOGIE

PAR
FELIPE RUST DE CARVALHO

MAI 2021

UNIVERSITÉ DU QUÉBEC À MONTRÉAL
Service des bibliothèques

Avertissement

La diffusion de ce mémoire se fait dans le respect des droits de son auteur, qui a signé le formulaire *Autorisation de reproduire et de diffuser un travail de recherche de cycles supérieurs* (SDU-522 – Rév.10-2015). Cette autorisation stipule que «conformément à l'article 11 du Règlement no 8 des études de cycles supérieurs, [l'auteur] concède à l'Université du Québec à Montréal une licence non exclusive d'utilisation et de publication de la totalité ou d'une partie importante de [son] travail de recherche pour des fins pédagogiques et non commerciales. Plus précisément, [l'auteur] autorise l'Université du Québec à Montréal à reproduire, diffuser, prêter, distribuer ou vendre des copies de [son] travail de recherche à des fins non commerciales sur quelque support que ce soit, y compris l'Internet. Cette licence et cette autorisation n'entraînent pas une renonciation de [la] part [de l'auteur] à [ses] droits moraux ni à [ses] droits de propriété intellectuelle. Sauf entente contraire, [l'auteur] conserve la liberté de diffuser et de commercialiser ou non ce travail dont [il] possède un exemplaire.»

ACKNOWLEDGEMENTS

First of all, I am grateful to everyone who has been with me throughout this moment of my life.

I am very grateful to my supervisor Paul A. del Giorgio for his guidance, patience, and scientific support. I am also thankful to you for the opportunity and having welcomed me in these last years and for always being understandable. Thank you for the moments of reflection and learning.

I am thankful to all funding agencies that have supported me or this project throughout these years. Thanks to Hydro Quebec and to Natural Sciences and Engineering Research Council of Canada (NSERC). I am also grateful to Yves Paire and Pascal Bodmer for the collaboration, support, and help throughout the last years.

Thanks to all colleagues and friends in Montréal. Thank you all for the support, it has been a great to spend these years in such diverse group. Thanks to Marie Geradin, Masumi Stadler, Ryan Hutchins, Michaela Melo, Mathilde Couturier, Naíla Barbosa, Sophie Crevecoeur, Cynthia Soued, Sofia Baliña, Teresa Aguirrezabala, Facundo Smufer, Mario Muscarella, Maximilian Lau, Pascal Bodmer, Joan Pere, Pedro Barbosa, Martin Demers, Jihyeon Kim, Amir Shahabinia, Yudhistir Reddy, Cindy Paquette, Vincent Fugère, Marie-Pier Hebert, Caroline Fink-Mercier, Tristy Vick-Majors, Candice Aulard, Tonya DelSontro, Leonardo Saggioro and François Banny. Thank you all for the support and unforgettable moments spent together.

I am also grateful to Alice and Serge for have helped in the sampling campaigns and in the data management, which are very important! Also to all summer students, especially Gabriel Bastien-Beaudet and Jean-Christophe Sicotte-Brisson.

I also would like to thank my family, for the love and support in all the difficulties, despite the distance. Lastly, thanks to Paulinha for the love, company and patience in many moments. I am lucky to have you with me! Te amo!

TABLE DES MATIÈRES

LISTE DES FIGURES.....	vii
LISTE DES TABLEAUX.....	ix
RÉSUMÉ	x
ABSTRACT	xi
INTRODUCTION	1
0.1 Litterature review.....	2
0.1.1 CO ₂ and CH ₄ in hydroelectric reservoirs: sources and pathways.....	2
0.1.2 Factors influencing spatial and temporal patterns of gases concentrations and emissions.....	5
0.2 Problem statment	7
0.2.1 Relevance of C emissions from hydroelectric reservoirs and current challenges	7
0.3 Thesis objectives and expected results	9
CHAPITRE I MODELING THE SPATIAL AND TEMPORAL TRENDS IN SURFACE CONCENTRATIONS OF CO ₂ AND CH ₄ IN A NEWLY CREATED COMPLEX OF HYDROELETCTRIC RESERVOIRS	10
1.1 Abstract.....	10
1.2 Introduction.....	11
1.3 Methods	17
1.3.1 Study site	17
1.3.2 Samping design	19
1.3.3 Enviromental and limnological parameters.....	20
1.3.4 CO ₂ and CH ₄ concentrations sampling collection.....	21
1.3.5 Other statistical analyses	25
1.4 Results	25

1.4.1	Temporal and spatial variability of measured CO ₂ and CH ₄ concentrations	25
1.4.2	Effects of spatial and temporal variables on CO ₂ and CH ₄ concentrations	31
1.4.3	Temporal and spatial variability of modeled CO ₂ and CH ₄ concentrations	34
1.5	Discussion	38
1.5.1	Temporal and spatial variability of measured CO ₂ and CH ₄ concentrations	39
1.5.2	Modeled CO ₂ and CH ₄ concentrations with remote available variables: effects and predictions	45
1.5.3	Implications of performed modeling approach	47
1.6	Conclusion	48
	ANNEXE A SUPPORT INFORMATION	50
	RÉFÉRENCES	58

LISTE DES FIGURES

Figure	Page
0.1. Conceptual schem of the carbon balance of hydroelectric reservoir.	5
1.1. Map of the geographical location of the sampling area, the La Romaine catchment, the main river and the location of three investigated reservoirs including their shape.....	18
1.2. Relationship between CO ₂ and CH ₄ concentrations in the three studied reservoirs. The dotted red lines indicate atmospheric CO ₂ (17 μM) and CH ₄ (0.003 μM) concentrations.....	26
1.3. Boxplot showing the temporal variability among sampled campaigns, reservoirs, and the La Romaine river (LR) of measured CO ₂ (left) and CH ₄ (right) concentrations. Boxplots represent median (black line), first and third quartiles (hinges), range (whiskers), and outliers (black dot). The dashed vertical lines represent mean annual concentrations of CO ₂ and CH ₄ , respectively.	28
1.4. Comparison of measured CO ₂ (left) and CH ₄ concentrations (right) of the surface, bottom and turbine intake of the three studied reservoirs. Boxplots represent median (black line), first and third quartiles (hinges), range (whiskers), and outliers (black dot). Lines represents regressions lines grouped by sampling site depth/location (colors match of the lines match with the colors of the boxplots).	29
1.5. Measured CO ₂ and CH ₄ concentrations from all the three reservoirs in August 2017. Figure is set in order of appearance in the cascade configuration. Each black dot represents a sampling site. The scales of the color bars are different from each other to better visualize spatial variabilities.	31

1.6. Measured and modeled CO ₂ and CH ₄ concentrations from all the three reservoirs. Each black dot represents a sampling site. The scales of the color bars are different from each other to better visualize spatial variabilities	35
1.7. Modeled concentrations of CO ₂ (left) and CH ₄ (right) over individual days in the ice free period. Each dot represents the modeled average of the CO ₂ and CH ₄ concentration in a day. Shaded polygons around the dots indicate 95% confidence interval for the mean. The square shape and error bars represents the measured CO ₂ and CH ₄ concentration (median and inter quartile range) of each sampled campaign.	36
S1.1. Figure showing the cascade reservoir configuration in the La Romaine river.....	52
S1.2. Relationship between measured and modeled water temperature	52
S1.3. Map of the La Romaine I dam showing the grid points (30 m x 30m) generated using the fishnet toolbox in ArcMap 10.....	53
S1.4. Regression tree showing the variability among seasons and reservoirs. of CO ₂ (A and C) and CH ₄ (C e D) concentrations.	54
S1.5. Scatterplot showing the daily average of CO ₂ and CH ₄ of the platform (grey dots) and our sampling sites (yellow dots and red dots). *Sample location next to the platform.	55
S1.6. Regression tree showing the relationship of depth and distance from shore of CO ₂ (A and B) and CH ₄ (C e D) concentrations.	56
S1.7 Rregression tree showing the relationship between the underlain land cover and CO ₂ concentrations in RO2 (A) and CH ₄ and CO ₂ concentrations (B e C, respectively) in RO1	57

LISTE DES TABLEAUX

Tableau	Page
1.1. Table showing the approach of previous studies	15
1.2. Background information of the three sampled reservoirs with the year of installation in parentheses.....	19
1.3. Fixed effects used to develop linear mixed effect models.	23
1.4. Results of linear mixed models, testing effects of the spatial and temporal variables on CO ₂ and CH ₄ concentrations in each of the three reservoirs. Site ID and sampling campaigns were included as a random effect on the intercept. Significances of fixed effects were assessed with likelihood ratio tests with degrees of freedom = 1. The slope direction (sign) of the effect is indicated with – or +.	33
S1.1. Limnological characteristics of the three investigated reservoirs. Average wind speed was measured at 1 m.....	51

RÉSUMÉ

Il a été établi que les réservoirs hydroélectriques émettent du dioxyde de carbone (CO_2) et du méthane (CH_4) vers l'atmosphère, mais il existe encore beaucoup d'incertitudes concernant l'amplitude et la régulation de ces émissions. Ces incertitudes sont particulièrement importantes les premières années suivant la mise en eau et dans les complexes de réservoirs en cascade où les études sont rares. Nous présentons ici les résultats d'une étude à grande échelle sur l'empreinte carbone du nouveau complexe La Romaine, le plus grand projet hydroélectrique en cours au Québec et en Amérique du Nord, qui est composé de trois réservoirs consécutifs dans la rivière La Romaine. Notre objectif principal a été la modélisation de la dynamique spatiale et temporelle des concentrations de CO_2 et de CH_4 dans les eaux de surface des trois réservoirs au cours des quatre premières années suivant la mise en eau. Les concentrations de CO_2 et de CH_4 dissous ont été intensivement mesurées sur trois saisons pendant quatre ans. Les résultats ont indiqué une augmentation instantanée des concentrations de CO_2 dans les trois réservoirs dès le début des mises en eau, avec toutefois des variations selon la saison, la morphométrie des réservoirs et la couverture terrestre. Les concentrations de CH_4 ont également augmenté dans les réservoirs par rapport aux conditions initiales de la rivière, mais les variations en lien avec les saisons et la morphométrie des réservoirs n'ont été observées qu'après plusieurs années suivant la mise en eau. De plus, les concentrations de gaz ont été stables au cours des premières années de mises en eau, à l'exception de la diminution des concentrations de CO_2 dans le réservoir peu profond RO1 et dans les couches profondes des réservoirs RO2 et RO3. Dans l'ensemble, les modèles développés ont reproduit relativement fidèlement les dynamiques spatiales et temporelles des concentrations mesurées de CO_2 et de CH_4 dans ce complexe hydroélectrique récemment créé. Les modèles ont mis en évidence les interactions de la saisonnalité, de la couverture terrestre et de la morphométrie des réservoirs dans la régulation des concentrations de CO_2 et de CH_4 . Ces informations améliorent notre compréhension globale des facteurs régulant la dynamique spatiale et temporelle de ces gaz dans les réservoirs boréaux, et permettent des estimations plus précises et représentatives des émissions diffuses de carbone de ces systèmes.

Mots clés : dioxyde de carbone, méthane, réservoirs hydroélectriques, dynamiques spatiale et temporelle, modélisation

ABSTRACT

It has been established that hydropower plants emit CO₂ and CH₄ to the atmosphere, yet there is still much uncertainty concerning the magnitude and the drivers of these emissions. Such uncertainty is particularly large over the initial years after flooding and in complex, cascade reservoir systems where studies are rare. Here we present results of a large-scale study on the carbon footprint of the newly created La Romaine complex, the largest ongoing hydroelectric project in Québec and in North America, which is composed of three consecutive reservoirs along La Romaine River. Our main objective was to model the spatio-temporal dynamics of CO₂ and CH₄ concentrations in the surface waters of all three reservoirs over the first four years after flooding. Both dissolved CO₂ and CH₄ concentrations were extensively measured over three seasons for four years. Results indicated an immediate upsurge in CO₂ concentrations in all three reservoirs from the onset of flooding, albeit with clear differences depending on the season, the reservoir morphometry and pre-flood land cover. CH₄ was also elevated in the reservoirs relative to the pre-flood river conditions, while also showing clear differences depending on the seasons and reservoirs morphometry, however only after a year lag after flooding. Moreover, surface water gas concentrations were stable over the initial years of flooding, with exception of the decrease in CO₂ concentrations in the shallower RO1 reservoir and in the deep layers of the two deep reservoirs (RO2 and RO3). Overall, the models developed here effectively reproduced the observed spatial and temporal patterns of CO₂ and CH₄ concentrations in this newly created hydroelectric complex, and highlighted the interaction of seasonality, land cover and reservoir morphometry in the regulation of CO₂ and CH₄ concentrations. This information increases our overall understanding of the drivers of the spatial and temporal dynamics of these gases in boreal reservoirs, combined with appropriate modeled gas transfer functions, it will yield more accurate and representative estimates of diffusive carbon emissions from these systems.

Keywords: CO₂, CH₄, hydroelectric reservoirs, spatio-temporal dynamics, modeling

INTRODUCTION

In the recent past, the role of inland aquatic ecosystems (rivers, lakes and reservoirs) in the global carbon (C) cycle has been neglected. These environments were sometimes considered to be simple terrestrial C transport routes to the oceans (IPCC, 2007). However, despite their small fraction of the Earth surface (Downing *et al.*, 2006; Lehner *et al.*, 2011), inland waters play an essential role in the C cycle of the continents (Cole *et al.*, 2007; Tranvik *et al.*, 2009). They are significant sources of the greenhouse gases (GHG) carbon dioxide (CO₂) and methane (CH₄) to the atmosphere (Bastviken *et al.*, 2011; Raymond *et al.*, 2013), and can meanwhile, bury more organic carbon (OC) in their sediments than the entire ocean (Aufdenkampe *et al.*, 2011; Tranvik *et al.*, 2009). Therefore, continental waters have the capability to process, stock and emit C, which may amount to 2 Pg C year⁻¹ (Cole *et al.*, 2007; Tranvik *et al.*, 2009).

Hydroelectric reservoirs have also been identified as significant C sources to the atmosphere (Barros *et al.*, 2011; Rudd, 1993; St Louis *et al.*, 2000) and C sink (Mendonça *et al.*, 2017). Hydroelectric reservoirs are human-made water impoundment, they represent one of the main human impacts on the hydrological cycle. The sea level has been reduced about 30 millimeters in the last 50 years as a consequence of new impoundments (Chao *et al.*, 2008). Thereby, these dams play an important role, their effect on landscapes and on the ecosystem dynamics are significant, since a river fragment is transformed into a completely distinct new system (Thornton, 1990). There are currently more than 1 million dams registered worldwide (Lehner *et al.*, 2011), 20% of which are used for electricity generation (ICOLD, 2016), yet this area is still expanding due to intense world energy demand

through the last decades. Therefore, although it is well established that most hydroelectric reservoirs emit significant amounts of CO₂ and CH₄ to the atmosphere (Barros *et al.*, 2011; Deemer *et al.*, 2016), our artificial lakes and reservoirs C understanding is still incomplete, mostly regarding their spatial and temporal dynamics (Deemer *et al.*, 2016), a better understanding of C processing in these environments may support global climate and C cycle models.

0.1 Litterature review

0.1.1 CO₂ and CH₄ in hydroelectric reservoirs: sources and pathways

It has been shown that hydroelectric reservoirs can have a double effect on the carbon (C) cycle (Mendonça *et al.*, 2012). Like most natural lakes, they are supersaturated in CO₂ (except for some eutrophic systems) and CH₄, acting as C sources to the atmosphere (Barros *et al.*, 2011). They can also act as carbon sinks (Mendonça *et al.*, 2017). They bury in their sediments the non-mineralized organic carbon (OC) and in eutrophic reservoirs, photosynthesis by the phytoplankton community consumes CO₂ lowering this gas concentration in the water column leading these systems to be atmospheric CO₂ sinks (Pacheco *et al.*, 2015). In fact, reservoirs acting as net C sinks occur all over the world, yet the number of reservoirs acting as net C emitting is larger (Barros *et al.*, 2011).

Commonly, CO₂ and CH₄ production and consumption routes are driven by aquatic metabolism. Aerobic and anaerobic respiration produces CO₂ which is consumed by photosynthetic organisms. On the other hand, CH₄ is produced by methanogens mostly under anoxia in sediments and can be consumed in hypoxic and oxic sediments and waters by methanotrophs (Conrad, 2009). An exception to this biological mediation is the C photochemical process, which the dissolved organic matter (DOM) is excited by UV and visible light. As a result the DOM is fragmented

in smaller molecules, which CO₂ the most abundant (Soumis *et al.*, 2007). Moreover, water column and sediments C dynamics are not the sole sources of these gases as CO₂ and CH₄ can also flow into reservoirs, either through the surface (e.g. tributaries) or via groundwater.

In general, the hydroelectric reservoirs CO₂ supersaturation is associated to the large amount of organic matter available to be mineralized, which results in an excess of heterotrophic respiration. This is the case especially in newly formed reservoirs, where the organic matter availability from the flooded surrounding vegetation is large, raising the respiration rate of planktonic or benthic aerobic bacteria (Abril *et al.*, 2005; Barros *et al.*, 2011). The mineralization can also occur anaerobically in the water column of stratified reservoirs and in their sediments (Abril *et al.*, 2014). When stratification occurs, the oxygen consumption in the deeper layers of reservoirs is not compensated by the water exchange with the upper layers which are usually well oxygenated. Thereby, the bottom waters gradually become anoxic. In an anoxic condition, methanogenic archaea metabolize organic compounds, such as acetate and CO₂ into CH₄ (methanogenesis), leading to high concentrations of CH₄ in the reservoir hypolimnia (Abril *et al.*, 2005). Moreover, in OC-rich sediments, CH₄ bubbles can be formed given the high mineralization rates combined with the hydrophobic characteristics of the CH₄ molecules. These bubbles tend either to be emitted to the atmosphere or dissolve in the water column (Bastviken *et al.*, 2004; Delsontro, T. *et al.*, 2010). However, significant amount of CH₄ produced may oxidize at the metalimnion into CO₂ by methanotrophs, before it gets emitted into the atmosphere. For example, oxidation in the water column of the Petit Saut reservoir reduced CH₄ emissions by more than 85% (Gu erin et Abril, 2007).

The excess gas relative to saturation resulted from both water column and sediment metabolisms tends to be emitted to the atmosphere. Carbon emissions from reservoirs (Figure 0.1) can occur mainly through:

(i) diffusive flux across the water-air interface (Roland *et al.*, 2010; Teodoru, C *et al.*, 2011). The diffusive flux at the water-atmosphere interface is dependent on both the water surface turbulence and the gradient in gas concentrations between these two compartments. It is straightforward calculated using the difference in gas concentration between the air and the water multiplied by the gas transfer velocity (k), as shown in equation 1 (Eq. 1).

$$\text{Gas flux} = k \times (\text{Conc.}_{\text{water}} - \text{Conc.}_{\text{air}}) \quad \text{Eq.1}$$

The concentrations can be measured by either a gas chromatograph or a portable gas analyser (LGR). The gas exchange coefficient k depends on water surface turbulence (Zappa *et al.*, 2007), and is mostly derived from empirical relationships with wind speed (Cole et Caraco, 1998). Alternatively, diffusive flux can be measured directly using floating chamber, however artificial turbulence generated by the chamber can affect the flux measurement (Vachon *et al.*, 2010).

(ii) Ebullition flux (bubbles) (Abe *et al.*, 2005; Delsontro, T. *et al.*, 2010); The ebullition flux is dominated by CH_4 and it occurs mostly in shallow reservoirs, whereas in deep reservoirs CH_4 bubbles usually dissolve in water before reaching the surface, since the bubbles release to the atmosphere is mostly controlled by hydrostatic pressure (Bastviken *et al.*, 2004).

iii) Water degassing during the turbine passage (Kemenes *et al.*, 2007) and/or (iv) water degassing in the downstream river (Guerin *et al.*, 2006). Hydroelectric reservoirs deep layers are rich in CO_2 and CH_4 , while the water passes through the turbines, these dissolved gases are exposed to a lower pressure, resulting in a rapid degassing to the atmosphere. Yet, large amounts of gases remain dissolved in the water and they can be found up to 40 km downstream from the dams (Guerin *et al.*, 2006).

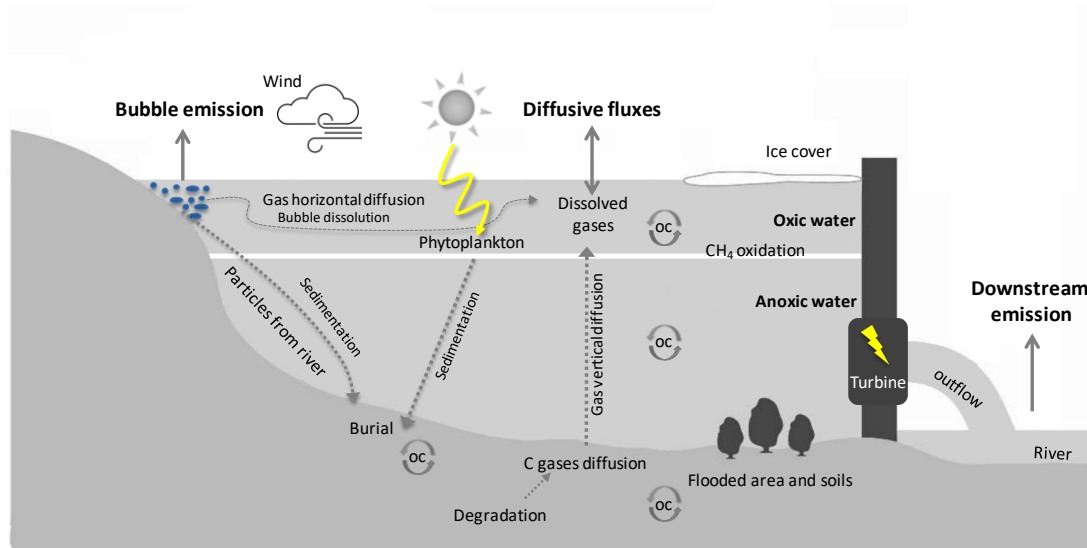


Figure 0.1. Conceptual schem of the carbon balance of hydroelectric reservoir.

0.1.2 Factors influencing spatial and temporal patterns of gases concentrations and emissions

Many factors are involved in controlling both CO₂ and CH₄ concentrations and emissions in reservoirs, hence a large degree of spatio-temporal variability on this fluxes has been observed both within and among reservoirs around the world (Deemer *et al.*, 2016). The large variability could be explained by the effect of the climate, the catchment characteristics, and also the morphometry of the reservoirs. Therefore, some processes and external factors influence within carbon concentrations and emission of hydroelectric reservoirs, such as reservoir morphometry, temperature, and flooded land cover.

For example, temperature can affect all processes involved in the production, consumption and emission of CO₂ and CH₄ in hydroelectric reservoirs. For instance, both aerobic respiration and primary production are temperature dependent (Flanagan et Syed, 2011; Sand-Jensen *et al.*, 2007). Although both process tend to be greater when the temperature is higher, it has been already shown that aerobic respiration is

more temperature dependent compared to primary production (Rivkin et Legendre, 2001; Sand-Jensen *et al.*, 2007). Thus, it is expected that higher rates of both process occur in either warmer seasons or climates (Lewis Jr, 2010). Moreover, both methanogenesis and metanotrophy are also temperature dependent (Chowdhury et Dick, 2013; Yvon-Durocher *et al.*, 2014). However, increase in temperature has a larger effect on CH₄ production than on CH₄ oxidation. Therefore, changes in temperature can lead inter-annual variability with higher emissions in warmer months (Lima, 2005). Temperature can also lead to among and within reservoirs variability: gas concentrations and emissions are usually higher in reservoir located in tropical areas (Barros *et al.*, 2011) and in regions within the reservoir, which the water temperature is warmer (Paraiba *et al.*, 2018). As a result of this positive relationship between C emissions and temperature, environmental changes related to temperature variations can affect the hydroelectric reservoir role as C sources to the atmosphere.

Reservoirs morphometry can also play a role in controlling the gases heterogeneity in the water column. It has been shown that riverine inflow areas, as well water depth were linked to gases. These areas had higher CO₂ and CH₄ concentrations, and therefore higher emissions than the main reservoir channel (Paranaiba *et al.*; 2018). Lastly, the pre-flooded landscape type can also be linked to the spatial heterogeneity of gas emissions. In this regard, different reservoir regions can show different C dynamics in the water column, due to the pre-flooded land type diversity. In fact, (Teodoru *et al.*, 2011) showed that part of the spatial variability of gas emissions can actually be explained and linked to the pre-flood landscape that characterize the different portions of the reservoir and its influences can last several years after flooding.

0.2 Problem statement

0.2.1 Relevance of C emissions from hydroelectric reservoirs and current challenges

Although hydropower is a renewable energy source, environmental impacts from these power plants can be significant (Fearnside, Philip M, 2001). Considerable consequences are observed when a river of flowing waters gives place to a reservoir - often larger, deeper and more stable. Typically, a hydroelectric development involves flooding a surrounding river area, and, as a result, the terrestrial vegetation that before acted as a carbon sink becomes available for decomposition by aquatic microorganisms, likely changing the local carbon dynamics. Moreover, the water residence time can increase from less than one day to several months, reducing the water velocity, decreasing the sediment transport capacity and also influencing the reservoir vertical patterns (Straskraba et Tundisi, 1999). Thus, a large amount of terrestrial organic material that would not be commonly processed or accumulated in the rivers tends to be in the reservoirs. For instance, organic matter deposited at the bottom of the reservoirs is more likely to be mineralized than if deposited on the ocean floor (Sobek *et al.*, 2009).

Notwithstanding, hydropower is the largest source of renewable energy, currently producing 24% of global electricity (ICOLD, 2016). Many northern countries use of some of their hydropower potential; for example, Canada is the third largest hydropower producer in the world, with hydropower accounting for 61% of the country's energy sources (NRC, 2013). In the province of Quebec, this contribution is even higher, with hydropower representing 99% of its energy sources (Hydro-Quebec, 2018). Quantifying anthropogenic C reservoir emissions into the atmosphere has become essential, given the growing global concern regarding both large energy demands and environmental issues. C emissions from hydroelectric reservoirs have been studied since the 90's, with the first scientific studies conducted in reservoirs

located in Canada (Duchemin *et al.*, 1995; Rudd, 1993). Over the last 25 years, studies have shown a major progress on our understanding of C processing and emissions from hydroelectric reservoirs. However, for a very long period, hydropower was commonly regarded a C-neutral energy source since it is renewable and does not release fossil carbon to the atmosphere (Hoffert *et al.*, 1998; Victor, 1998). This has generated an intense discussion on C emissions in reservoirs, which is still not settled (dos Santos *et al.*, 2017; Fearnside, P. M., 2006; Fearnside, Philip M. et Pueyo, 2012; Giles, 2006; Rosa *et al.*, 2004). However, nowadays it is acknowledged that many hydroelectric reservoirs can contribute with relatively large amounts of C to the atmosphere (Barros *et al.*, 2011).

Nonetheless, this debate is still open, current estimates from reservoirs (Barros *et al.*, 2011; Deemer *et al.*, 2016; St Louis *et al.*, 2000) differ by more than one order of magnitude. Mostly due to the lack of uniform sampling and estimation approaches worldwide, it is noticeable that not all studies have presented the same methodology regarding sampling design, gas measurements and gas flux estimations (Deemer *et al.*, 2016). As consequence, this triggers to a greater uncertainty in estimating local and global C emissions, either underestimating or overestimating the emissions. Thus, in order to assess the carbon budget of hydroelectric reservoirs, obtaining accurate estimates of diffusive gas emission is the first step and one of the key factors needed. As mentioned previously, diffusive emission is straightforward calculated using equation 1. Nevertheless, quantifying accurately these diffusive emissions are not trivial, issues such as remoteness, difficulty of access and sampling of large and complex water bodies are major challenges. These emissions are often highly variable in both space and time, varying up to several order of magnitude even within a single reservoir and from season to season. Therefore, in order to enable more precise estimates of the hydroelectric reservoirs influence on both regional and global C cycle, it is necessary to answer questions that have remained unanswered on the studies that have been carried out. Future studies have to consider approaches that

explicitly incorporate information from reservoir's regions that are not often sampled (bays, river inlets) and integrate them temporarily. Underestimation of emission due to neglect of spatial variability can be considerable, as it has been shown that reservoir shallow areas are emission hotspots (Paranaíba *et al.*, 2018; Sobek *et al.*, 2012). Thus, estimates that integrate spatial and temporal factors to (i) account for the high spatial and temporal variability in the gases distribution within and among reservoirs; and (ii) that extrapolate individual measurements to the entire system and over time, could represent the best alternative to improve our understanding of the actual dynamics of these impoundments on the anthropogenic greenhouse gas emissions into the atmosphere.

0.3 Thesis objectives and expected results

To address some of these challenges, the overall objective of this thesis was to investigate the dynamics of CO₂ and CH₄ concentrations during the initial years of three boreal hydroelectric reservoirs built in a cascade configuration in the La Romaine River (Canada, QC). More specifically, we aimed to use point measurements to develop and apply empirical models of dissolved gases (CO₂ and CH₄) concentrations that integrate spatial and temporal factors. Our approach was to use both temporally and spatially remotely available variables to manage issues such as remoteness, difficulty of access and sampling of large and complex water bodies. As result, we were expecting to reduce the uncertainty yielded by estimating emissions based solely on averaging point measurements. Overall, this thesis should enable us to provide a unique scientific understanding of C concentrations in a series of cascaded reservoirs, especially during the critical initial years after flooding. Ultimately, we expect to improve estimates of CO₂ and CH₄ concentrations and therefore emissions from hydroelectric reservoirs of different characteristics. Also increase our overall understanding of both spatial distribution and temporal dynamics of these gases in these environments.

CHAPITRE I

MODELING THE SPATIAL AND TEMPORAL TRENDS IN SURFACE CONCENTRATIONS OF CO₂ AND CH₄ IN A NEWLY CREATED COMPLEX OF HYDROELECTRIC RESERVOIRS

1.1 Abstract

It is well established that hydroelectric reservoirs emit greenhouse gases such as carbon dioxide (CO₂) and methane (CH₄) to the atmosphere, yet there is still much uncertainty concerning the magnitude and the drivers of these emissions. Such uncertainty is particularly large over the initial years after flooding and in complex, cascade reservoir systems where studies are rare. We studied the newly created La Romaine complex, the largest ongoing hydroelectric project in Québec and in North America, which is composed of three consecutive reservoirs along La Romaine River (RO1, RO2, RO3). Our main objective was to model via remotely available input data the spatio-temporal dynamics of CO₂ and CH₄ concentrations in the surface waters of all three reservoirs over the first four years after flooding. Both, dissolved CO₂ and CH₄ concentrations were extensively measured over three seasons for four years. Results show an immediate upsurge in CO₂ concentrations in all three reservoirs from the onset of flooding, albeit with clear differences depending on the season, the reservoir morphometry and pre-flood land cover. CH₄ concentrations were also elevated in the reservoirs relative to the pre-flood river conditions but only

after a year lag after flooding, also with clear seasonal differences and a dependence on reservoirs morphometry. CO₂ and CH₄ concentrations were relatively stable over the initial years of flooding, with exception of the decrease in CO₂ concentrations in the shallower RO1 reservoir and in the deep layers of deep reservoirs (RO2 and RO3). Overall, the models developed here effectively reproduced the observed spatial and temporal patterns of CO₂ and CH₄ concentrations in this newly created hydroelectric complex, and highlighted the interaction of seasonality, land cover and reservoir morphometry in the regulation of surface water CO₂ and CH₄ concentrations. Combined with appropriate modeled gas transfer functions, the models will contribute to more accurate and representative estimates of diffusive carbon emissions from boreal reservoirs, and also increases our overall understanding of the drivers of the spatial and temporal dynamics of greenhouse gases in these systems.

1.2 Introduction

It is well established that hydroelectric reservoirs emit significant amounts of the two major greenhouse gases (GHG), carbon dioxide (CO₂) and methane (CH₄), to the atmosphere (Abril *et al.*, 2005; Barros *et al.*, 2011; Deemer *et al.*, 2016; Fearnside, P. M., 2006; Kemenes *et al.*, 2007; Rosa *et al.*, 2006; Rudd, 1993). Over the past decade there has been an increasing awareness that these emissions associated to the creation of reservoirs for the generation of hydroelectricity and other uses need to be quantified and accounted for (Deemer *et al.*, 2016). More recently, there has been calls to explicitly include reservoir emissions in national carbon (C) inventories, and to consider GHG emissions in the design and management of hydroelectric reservoirs (Fearnside, Philip M., 2015). These developments all highlight the need to improve the current estimates of reservoir GHG emissions, and the models used to predict future emissions (Prairie *et al.*, 2018). These emissions occur mainly through three main pathways: (i) diffusive flux across the water-air interface (Roland *et al.*, 2010; Teodoru, C *et al.*, 2011) ; (ii) ebullition flux (bubbles) (Abe *et al.*, 2005; Delsontro, T.

et al., 2010); and (iii) water degassing during the turbine passage and in the downstream river (Guerin *et al.*, 2006; Kemenes *et al.*, 2007). The relative importance of the three pathways varies with reservoir size, morphometry and geographic location (Prairie *et al.*, 2018), and each pathway has its own set of drivers and needs to be quantified, understood and modeled separately in order to improve the overall carbon footprint of reservoirs.

One of the key factors need to evaluate the overall carbon footprint of reservoir is to obtain accurate estimates of diffusive emissions. However, these emissions are often highly variable in both space and time, as they can vary in orders of magnitude in space and in time even within a single reservoir. For example, diffusive emission of CH₄ varied spatially from 0.012 to 258 mg C m⁻² day⁻¹ in a tropical reservoir (Paranaíba *et al.*, 2018), and a similar range in spatial variability was also observed in a boreal reservoir where CO₂ emissions ranged from 1760 up to 14200 mg C m⁻² day⁻¹ (Teodoru, C *et al.*, 2011). A recent global scale review (Deemer *et al.*, 2016) showed that CH₄ fluxes (diffusive and ebullitive) across all types of reservoirs can vary up to 4 orders of magnitude. Multiple factors are involved in controlling both CO₂ and CH₄ concentrations and the resulting fluxes in reservoirs. Some of the variability in C emissions may be explained by the effect of internal and external factors, such as regional climate, reservoir morphometry, and the catchment characteristics (Mendonça *et al.*, 2012). For example, temperature in particular affects most processes involved in the production and consumption of CO₂ and CH₄ in aquatic systems. Both aerobic respiration and methanogenesis are temperature dependent (Chowdhury et Dick, 2013; Flanagan et Syed, 2011), but to different extent (Sand-Jensen *et al.*, 2007; Yvon-Durocher *et al.*, 2014). Therefore, variations in temperature can lead to seasonal and inter-annual variability with higher C concentrations and emissions generally recorded in warmer months (Lima, 2005). Moreover, it has been shown that C concentrations and emissions are usually higher in reservoirs located in tropical areas (Barros *et al.*, 2011). Variations in temperature

can also be observed regarding the seasonal variability, although only few studies show season scale reservoir C emissions data (Deemer *et al.*, 2016). For example, in subtropical reservoirs diffusive CO₂ fluxes were higher in colder seasons (Wang *et al.*, 2015; Wang *et al.*, 2011) compared to warm seasons. Similarly, in a boreal reservoir, diffusive CO₂ emissions were higher in spring due to the winter CO₂ buildup under the ice cover, while diffusive CH₄ emissions were higher during summer due to higher water temperature (Bastien *et al.*, 2011). Therefore, not taking seasonality into consideration may either under or overestimate annual-scale fluxes. Internal factors, such as reservoir morphometry, play a key role in controlling the spatial heterogeneity in gas concentrations in the water column, because they determine, among other things, the extent of contact between pelagic, littoral and benthic components. It has been shown that water depth and riverine inflow areas, are as well linked to gas dynamics. These areas tend to have higher CO₂ and CH₄ concentrations, and therefore higher emissions than the main reservoir channel (Paranaíba *et al.*, 2018). Moreover, different reservoir locations can show different C dynamics in the water column due to the pre-flooded land physiognomy. Part of the spatial variability of gas emissions can actually be explained by the pre-flood landscape that characterize the different portions of the reservoir and this influences can last several years after flooding (Teodoru, C *et al.*, 2011)

These factors result in often a large degree of both spatial and temporal variability in CO₂ and CH₄ concentrations, in both surface and deep reservoir waters, and therefore fluxes. This variability is exacerbated in reservoirs that have a large surface, have flooded watersheds with heterogenous landcover and physiognomy, that have complex morphometries due to local topography, and that experience wide seasonal climatic shifts. In addition, the drivers of the production of CO₂ and CH₄ are not necessarily the same, and they are often only weakly coupled in time and space (Denfeld *et al.*, 2020), such that each gas needs to be assessed separately. Thus, it is clear that in order to robustly determine the C reservoir emissions, it is essential to

account for the heterogeneity in the gases (Paranaíba *et al.*; 2018). In this regard, previous studies have applied a range of sampling and methodological approaches in order to address the issue of ambient gas heterogeneity, and Table 1.1 summarizes several examples. It is clear that sampling intensity, both spatial and temporal, varies greatly among studies, ranging from having a few discrete sampling points to a continuous sampling scheme, some considering seasonality while others do not (Table 1.1). This heterogeneity in approaches adds to the overall uncertainty in current local and global estimates of reservoir C emissions (Deemer *et al.*, 2016). For example, Abril *et al.* (2005) showed that for a tropical reservoir, sampling a single point assumed to be representative of the entire reservoir resulted in an underestimation of CH₄ by 50% and CO₂ by 30%.

Table 1.1. Table showing the approach of previous studies

Study	Region	Gas species	Num. of Reservoirs	Num. of Sites	Sampled seasons	Sampling method	Flux upscaling approach
Duchemin et al., 1995	Boreal	CO ₂ , CH ₄	2	11	Spring Summer	Chambers	Average
Teodoru et al., 2011	Boreal	CO ₂ , CH ₄	1	40	Winter Autumn Spring Summer	Chambers Headspace-technique	Average
Soumis et al., 2004	Temperate	CO ₂ , CH ₄	6	24	Summer	Chambers	Average
Shi et al., 2017	Sub-tropical	CO ₂ , CH ₄	6	23	Summer	Headspace technique	Average
Galy-Lacaux et al., 1997	Tropical	CO ₂ , CH ₄	1	3	Spring, Summer Autumn	Chambers	Average
Abril et al., 2005	Tropical	CO ₂ , CH ₄	1	1-8	Autumn Summer*	Chambers and headspace technique	Average
Roland et al., 2010	Tropical	CO ₂	5	**	Summe* Winter	Equilibrator-Based (infrared gas analyzer)	Interpolation (kriging) Average
Paranaíba et al., 2018	Tropical	CO ₂ , aCH ₄	3	***	Winter	Equilibrator-Based (UGGA) Headspace-technique	Interpolation (IDW) Average
Soued & Praire 2020	Tropical	CO ₂ , CH ₄	1	39	Winter Spring Autumn	Chambers	Average Modeling****

* Gas concentrations were measured at irregular intervals in 1994 and 1995 in a specific site (from 3 to 10 times a year depending on parameters) and a more intensive monthly monitoring started in 1996 with few exceptions.

** pCO₂ samples were taken at approximately every kilometer along the length of the reservoir.

*** They used an online equilibration system connected to an ultraportable greenhouse gas analyzer (UGGA) to perform continuous measurements of pCO₂ and pCH₄ in the water as the boat moved (7 km h⁻¹) through the reservoirs. Headspace technique was done in 66 sites in total at the 3 reservoirs sampled, with triplicate measurements at each site.

**** The measured data of the C emissions of Batang Ai was compared to values derived from the G-res model (UNESCO/IHA, 2017) and the model presented in Barros et al. (2011).

Here we present a large-scale study of dissolved gas concentrations (CO_2 and CH_4) within three reservoirs of the newly created La Romaine hydroelectric complex, the largest ongoing hydroelectric project in Canada and in North America, which will eventually be composed of 4 consecutive reservoirs along La Romaine River in North Eastern Québec (Canada). The reservoirs are in a cascade configuration and in close proximity, they share the same water source and general regional climate but differ in size and morphometry as well as in the relative composition of the landscape types that were flooded within the basin. This allows us to assess the patterns of spatial and temporal heterogeneity in CO_2 and CH_4 under different reservoir configurations but similar climate and water chemistry, and identify the underlying drivers of this variability. We present the results of a 4-year study where we assessed both the spatial and temporal variability of CO_2 and CH_4 concentrations in the surface and deep waters of the three existing reservoirs over the initial years after flooding. On the basis of these observations we developed empirical models that link ambient gas concentrations to climate and remotely available variables, which provide both insight on the drivers and controls of gas concentrations in these reservoirs and also tools to derive a spatially explicit cartography of gas concentrations that accounts for seasonality as well as for reservoir age. The latter is necessary in order to reduce the uncertainty involved in deriving fluxes from individual point measurements in highly heterogeneous reservoirs. Our overall objective is to improve estimates of CO_2 and CH_4 concentrations in these newly created hydroelectric complex, which combined with appropriate modeled gas transfer functions, will eventually yield more accurate and representative estimates of diffusive GHG emissions for these reservoirs and contribute to the development of robust overall C footprints for the entire complex. The modeling also increases our overall understanding of the drivers of both spatial distribution and of the temporal dynamics of these gases in these major boreal reservoirs.

1.3 Methods

1.3.1 Study site

The study was conducted in the La Romaine hydroelectric reservoir complex (Figure 1.1 and Figure S1.1). It is located in the La Romaine river (Strahler stream order 8) situated on the North shore of the Gulf of St Lawrence in the boreal Côte-Nord region in Québec, Canada. The reservoirs lie over the physiographic unit of the Laurentian Plateau (<https://atlas.gc.ca/phys>), this region is characterized by rocky hills that can reach around 300 m in height, these steep stretches feature a series of waterfalls and rapids. This area is mostly covered by coniferous forest (45%), which black spruce-moss is the most abundant. Mixed stands (13.6%), broadleaf forest (3.6%), shrub (1.5%) and Wetland (0.4%) are less abundant ((Hydro-Québec, 2008).

The La Romaine river, which is the major water source for all three studied reservoirs, drains an area of almost 14,500 km² and travels nearly 500 km from the outlet of a chain of major headwater lakes (Figure 1.1). The water of the river vary little along its length, it is humic, slightly acid, iron-rich, nutrient-poor and carries little suspended matter (Hydro-Québec, 2008). The ice cover starts forming in early December and starts to break in late-April, in the period from June and September the mean water temperature is around 14°C with a mean peak around 22°C between July and August. The region mean annual air temperature is -2°C and the annual mean precipitation is 940 mm (Hydro-Québec, 2008).

The current complex consists of three hydroelectric power plants that were commissioned between 2014 and 2017. To date, the following reservoirs have been installed: La Romaine I (RO1; December 2015), La Romaine II (RO2; December 2014) and La Romaine III (RO3; May 2017). A fourth reservoir (RO4) was planned to be commissioned in 2020, but is not included in this study. The total installed

capacity is 1550 MW and an annual output of 8.0 TWh (www.hydroquebec.com/romaine/). The main characteristics of the three reservoirs are summarized in Table 1.2 and Table S1.1.

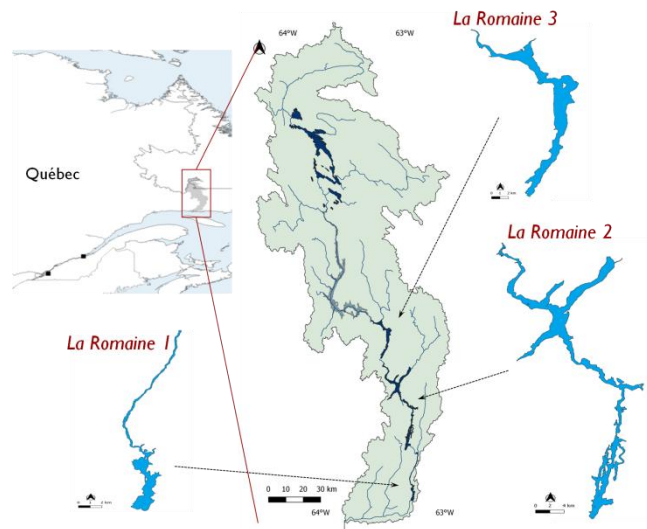


Figure 1.1. Map of the geographical location of the sampling area, the La Romaine catchment, the main river and the location of three investigated reservoirs including their shape.

Table 1.2. Background information of the three sampled reservoirs with the year of installation in parentheses.

	La Romaine I (RO1 - 2016)	La Romaine II (RO2- 2014)	La Romaine III (RO3 - 2017)
Dam height (m)	37.6	109	95
Turbine water intake (m)	19.5	45.4	37.4
Mean water depth (m)	22	61	67
Installed power (MW)	270	640	395
Area (km ²)	12.6	85.8	38.6
*Water/Exposed land (%)	47.3	17.5	22.8
*Wetland (%)	1	0.1	0
*Bryoids (%)	3.9	1	0
*Shrub (%)	3.1	0.9	0.7
*Broadleaf (%)	6.7	3	0.4
Mixedwood (%)	20.8	16.5	2.7
Coniferous (%)	17.2	61	73.4

* Percentage of flooded land cover

1.3.2 Sampling design

In total we have performed 11 field campaigns between 2015 and 2018. For all sampling campaigns combined, samples were taken in 150 unique sites across all three reservoirs which were sampled several times over the studied period, for a total of 734 individual observations (305 in RO1, 378 in RO2 and 51 in RO3). To capture the seasonal variability of these systems, field campaigns were conducted over 20 days three times per year during the ice free period (May to November), in the months of June (spring), August (summer) and October (autumn), except in 2015, when only two campaigns were carried out (June and in August). Furthermore, in order to capture the spatial variability within the reservoirs, 45% of all investigated sites were located at the littoral (< 10 m deep), 25% in the semi-pelagic area (10 - 20

m deep), and 30% in the pelagic zone. Moreover, bottom water samples were taken using a Van Dorn bottle (Alpha™, WildCO, USA) in every campaign at the dam region in all reservoirs. In RO1 the deep samples were taken at 28 m deep and in both RO2 and RO3 at 60 m. Partial pressure of CH₄ and CO₂ (pCH₄ and pCO₂) was sampled and calculated as explained below for surface water samples. Sampling of RO1 and the lower portion of RO2 was carried out by boat, whereas the upper portion of RO2, RO3 and the upper rivers portions were sampled by hydroplane. In addition to the discrete sampling, there was a floating autonomous measuring platform installed in the main channel of RO2 that yielded continuous surface water measurements of pCH₄ and pCO₂ for the ice free period, and there were systems installed in each of the three power stations taking continuous measurements of pCO₂ and pCH₄ of the water flowing through the turbines (details below in section 1.3.4).

1.3.3 Environmental and limnological parameters

At each sampling site, surface water temperature (°C), conductivity (μS cm⁻¹), pH, and dissolved oxygen (O₂) saturation (%) were determined using a multiparameter probe (600XLV2-M, Yellow Springs Instruments, OH, USA). We also measured air temperature and wind speed at 1 m above the water surface with a handheld weather meter (Kestrel Meter 4000, PA, USA). In addition, surface water samples were collected using polypropylene bottles (5 L) at each sampling site, processed the same day and stored frozen until analysis. Samples were analyzed for chlorophyll *a* (Chl_a: μg L⁻¹), total phosphorus (TP: μg L⁻¹), total nitrogen (TN: mg L⁻¹), dissolved organic carbon (DOC: mg L⁻¹), and dissolved inorganic carbon (DIC: mg L⁻¹) in the GRIL's (Groupe de recherche interuniversitaire en limnologie) analytical laboratory at the Université du Québec à Montréal, Montreal, Québec, Canada. Chl_a was filtered (GF/F, Whatman, Kent, UK) and extracted with ethanol (90%) and determined after acidification by spectrophotometry (665 and 750 nm, Ultrospec 2100 pro, Thermo Fisher Scientific Inc., Waltham, MA, USA). TP and TN samples were analyzed by

spectrophotometry following potassium persulfate digestion (Ultrospec 2100 pro, Biochrom Ltd., Cambridge, UK) and alkaline persulfate digestion (O I Analytical, College Station, TX, USA), respectively. Finally, DOC and DIC samples were filtered through 0.45- μm polyethersulfone cartridges (Sarstedt AG & Co., Germany) and stored at 4° and dark until measurement using high-temperature persulfate oxidation on a total carbon analyzer (TOC1010, OI Analytical, USA).

1.3.4 CO₂ and CH₄ concentrations sampling collection

Samples to determine the ambient pCH₄ and pCO₂ were taken at each site using the headspace technique (Kling *et al.*, 1991). We collected water in 1L plastic bottles (Thermo Scientific™, Nalgene™ Square, USA) at 10 cm below the water surface, and removed 500 mL of water replacing it with zero air (AI 0.0UM, Praxair, Inc., Canada) using a peristaltic pump (Masterflex E/S Portable Sampler, USA) to create a headspace. Bottles were shaken for minimum two minutes to equilibrate the water- and air phases inside the bottle. The gas phase was then pumped back into an air-tight aluminum foil bag and pCO₂ and pCH₄ were measured in the same day in the field laboratory with an ultraportable greenhouse gas analyzer (UGGA, Los Gatos Research, Inc., USA). Both CO₂ and CH₄ concentrations were calculated by multiplying the respective gas partial pressure sampled at each site with the in situ temperature adjusted Henry's law coefficient (Weiss, 1970; Wiesenburg et Guinasso, 1979).

Continuous gas measurements at turbine intake and float dock

Hydro-Quebec had installed automated systems (Bastien *et al.*, 2009) to measure continuously pCO₂ and pCH₄ at each reservoir generating station and one in a floating dock at the main channel in RO2 (Latitude: 50°31'31.2" N, Longitude: 63°15'02.8"). pCO₂ and pCH₄ were measured in the turbines and floating dock using

a combination of a portable CO₂ (LI-820 CO₂ Analyzer, LI-COR, USA) and CH₄ analyzer (Panterra, Neodym Technologies, Canada). Each of the automated systems was connected to a water circulating system and a gas extraction module, the samples at the floating dock were taken at 0.5 meter water depth. pCO₂ and pCH₄ was measured every three hours for the following periods: (1) RO1 from August 2016 to December 2018; (2) RO2 from February 2015 to December 2018; (3) RO3 from December 2017 to December 2018; (4) floating dock at RO2 from June 23 to October 15 in 2015, and from June 21 to October 16 in 2018.

Modeling approach

Model development

We developed linear mixed effect models (LMM) to evaluate and predict the effects of spatial and temporal variables (Table 1.3) on the response variables CO₂ and CH₄ concentrations in individual reservoirs using the `lmer()` function of the package ‘lme4’ (Bates *et al.*, 2015). To facilitate the development of predictive models, especially in the case of this type of remote reservoirs with difficult access, we chose to develop the LMM using only remotely available variables (Table 1.3). We chose LMM because it has the advantage of fitting autocorrelated (spatially and temporally) data (Bolker, 2015). Hence, site ID and field campaigns were considered as random effects.

Model selection was done using likelihood ratio chi-squared tests using `anova()` function. First we built models containing all variables (full models) and compared these with reduced models in which we gradually dropped variables. Thus, variables that had no effect on dependent variables were removed. The selected model was then compared with a totally reduced model (without fixed effects) in order to validate whether it was statistically different. The models selection was followed by a model validation, checking the residuals for normal distribution and homogeneity of

variances. CH₄ concentration was log-transformed to meet normality and homoscedasticity of residuals.

Table 1.3. Fixed effects used to develop linear mixed effect models.

Category	Variable	Data source	Method
Spatial	Site depth	Our survey	Depth meter (Speedtech SM-5)
Spatial	Site distance from shore	Our survey	ArcGis 10.1
Spatial	Site underlying land cover type	GeoGratis ¹	ArcGis 10.1
Temporal	Water temperature	Our survey & meteorological station ²	Modeled using air temperature
Temporal	Day of year	Our survey	³
Temporal	Age of the reservoir	Our survey	⁴

¹ <http://geogratias.cgdi.gc.ca> (access date: 13/10/2019)

² Latitude: 50°16'55" N, Longitude:63°36'41.0", <https://climate.weather.gc.ca> (access date: 20/12/2019)

³ Day of year that the sampling site was sampled

⁴ Calculated in decimal years from the reservoir flooding

Data preparation for modeling approach

For the spatial variables (Table 1.3), the sampled watershed was delineated using the *hydrology* tool (ArcGIS). The underlying land cover type (coniferous, broadleaf, mixed wood, shrub, wetland, exposed land and water) was determined for each site for all the reservoirs using land cover maps (30 m x 30 m) obtained from GeoGratis (<http://geogratias.cgdi.gc.ca/>). Site depth was measured with a depth meter (Laylin Speedtech SM-5, USA). Site distance from shore was calculated using *near* tool

(ArcGIS). All geospatial analyses were performed in ArcMap (version 10.1, Esri, USA).

For the temporal variables (Table 1.3), the age of the reservoirs was calculated in decimal years from each respective reservoir flooding. Water temperature was modeled using the measured surface water temperatures using a polynomial regression based on a 42-day moving average of daily air temperature and on the day of the year ($R^2 = 0.91$, $p < 0.0001$,

Figure S1.2). The daily air temperature was obtained from a meteorological weather station located at 28 km from RO1, 48 km from RO2, and 96 km from RO3 (Latitude: $50^{\circ}16'55''$ N, Longitude: $63^{\circ}36'41.0''$, <https://climate.weather.gc.ca/>). Average daily air temperature was calculated using hourly temperature measurements between the sunrise and sunset, since we sampled only during the day. We used `getSunlightTimes()` function of the package ‘`suncalc`’ to retrieve sunrise and sunset times (Benoit et Achraf, 2019). Modeled water temperatures were used to predict the dissolved CO_2 and CH_4 concentrations rather than the measured water temperatures because we aimed at using only remote available variables.

Application of the developed models

We used the empirical models described above to extrapolate the gas concentrations to areas and days which were not sampled, and to do this we generated a new dataset containing new georeferenced data points with all the model’s fixed effects, over the ice-free period and across the entire surface of each of the three reservoirs. First, we created a georeferenced points grid using *fishnet* toolbox in ArcMap 10.1 (Figure S1.3) covering all reservoir surfaces with the maximum resolution possible (same as data file with the lowest resolution, i.e. land cover type, 30 m x 30 m), and as a result we generated 152 151 data points across the surface of all three reservoirs. For each

of these data points were assigned a site underlying land cover type, distance from shore, water temperature, day of year, reservoir age and a maximum site depth which was obtained developing bathymetric analysis by the difference between before and after the flooding of the reservoirs, using a digital elevation model (resolution of 23 m x 23 m, obtained from GeoGratis). Moreover, to apply the model in the newly created dataset we used the prediction() function of the package 'lme4' (Bates et al., 2015).

1.3.5 Other statistical analyses

We used regression tree analysis to identify and describe temporal and spatial patterns in the CO₂ and CH₄ concentration among seasons as well as within and among the reservoirs. We used the rpart() function of the package 'rpart' (Therneau *et al.*, 2019). Linear regressions were performed to examine correlations between CO₂ and CH₄ concentrations in the three studied reservoirs and also correlations between the measured CO₂ and CH₄ concentrations from the surface, bottom and turbine inlet. The reported R² values are adjusted for the number of data points. The significance of the regression slope was tested by analysis of variance (ANOVA) at a significance level (p) of 0.05. All modeling and statistical exercises were performed in R version 3.6.0 (R Core Team, 2018).

1.4 Results

1.4.1 Temporal and spatial variability of measured CO₂ and CH₄ concentrations

The surface waters from all three reservoirs were consistently supersaturated in CO₂ and CH₄ relative to the atmospheric (Figure 1.2). CO₂ and CH₄ concentrations were only very weakly correlated to each other (R² = 0.02, p = 0.0003), and varied over up to 3 orders of magnitude across all three reservoirs and in time (Figure 1.2). The CO₂ concentrations ranged from 22 to 200 μM in RO1 (mean ± SD: 80 ± 29 μM), from 19

to 202 μM in RO2 ($75 \pm 38 \mu\text{M}$), and from 39 to 95 μM in RO3 ($58 \pm 13 \mu\text{M}$). The CH_4 concentration ranged from 0.004 to 5.2 μM in RO1 ($0.5 \pm 0.7 \mu\text{M}$), from 0.007 to 2.1 μM in RO2 ($0.14 \pm 0.16 \mu\text{M}$), and from 0.014 to 0.67 μM in RO3 ($0.12 \pm 0.13 \mu\text{M}$).

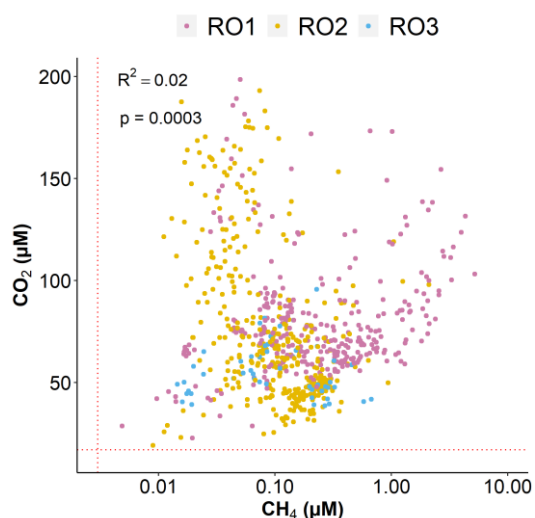


Figure 1.2. Relationship between CO_2 and CH_4 concentrations in the three studied reservoirs. The dotted red lines indicate atmospheric CO_2 (17 μM) and CH_4 (0.003 μM) concentrations.

There was a clear seasonal variability in the CO_2 and CH_4 concentrations in the sampled reservoirs (Figure 1.3), significant differences in both CO_2 and CH_4 concentrations were observed between seasons ($p < 0.001$, Figure S1.4). In general, CO_2 concentrations were on average highest in the spring (mean \pm SD: $105 \pm 44 \mu\text{M}$), with a clear decrease towards the summer (mean \pm SD: $60 \pm 24 \mu\text{M}$). CH_4 concentrations showed a clearer pattern than CO_2 among the reservoirs, and were in all three reservoirs always highest in the summer ($0.4 \pm 0.6 \mu\text{M}$), with the lowest average concentrations observed in the spring ($0.15 \pm 0.2 \mu\text{M}$). Moreover, the upstream river followed the same seasonal CO_2 and CH_4 concentration dynamics observed in the reservoirs (Fig. 1.3), where CO_2 concentrations were slightly higher

in the spring campaigns (mean \pm SD: $40 \pm 10 \mu\text{M}$) compared with summer ($27 \pm 3.7 \mu\text{M}$), and CH_4 concentrations were slightly higher in the summer campaigns ($0.05 \pm 0.03 \mu\text{M}$) compared with spring ($0.02 \pm 0.01 \mu\text{M}$).

A comparison of our point sampling of surface water CO_2 and CH_4 concentrations with the continuous sampling by the automated system in the floating dock deployed in the RO2 reservoir that measured surface CO_2 and CH_4 concentrations every three hours, showed similar average values along the open water season (Figure S1.5). For example, the average CO_2 concentration over the summer measured in the platform was $54 \pm 9.7 \mu\text{M}$ whereas the average in our sampling sites was $47 \pm 8.8 \mu\text{M}$ (all sites included). For CH_4 , the average concentration in the platform was 1.9 ± 1.6 and in our sampling sites it was $2.2 \pm 1.0 \mu\text{M}$.

CO_2 concentrations in the deeper layers of RO2 and RO3 were on average significantly higher than in the surface layer, which was not the case for shallower RO1, but concentrations of CH_4 were roughly similar between surface and deeper layer in all three reservoirs (Figure 1.4). There were generally no significant differences in both surface water CO_2 and CH_4 concentrations among the years sampled ($p > 0.05$, Figure 1.3), except in RO1, where the average CO_2 concentration sampled in 2018 ($69 \pm 20 \mu\text{M}$) was significant lower ($p < 0.001$) than the average CO_2 concentrations sampled in both 2016 ($90 \pm 38 \mu\text{M}$) and 2017 ($114 \pm 26 \mu\text{M}$). Interestingly, the deeper waters followed a strikingly different temporal dynamics than in surface waters in RO2, where the CO_2 concentrations measured at the turbine inflow clearly decreased over the years ($R^2 = 0.28$, $p = 0.008$), as did the concentrations measured in deeper sites through discrete sampling ($R^2 = 0.48$, $p = 0.002$, Figure 1.4). The concentration of CO_2 also declined in the deep layers of RO1 but paralleling the decline observed in surface water concentrations (Figure 1.4). There are only 2 years of data for RO3, so not clear inter-annual trend could yet be

established for this reservoir, although we can observe a slightly decrease in CO_2 concentration over the 2 years.

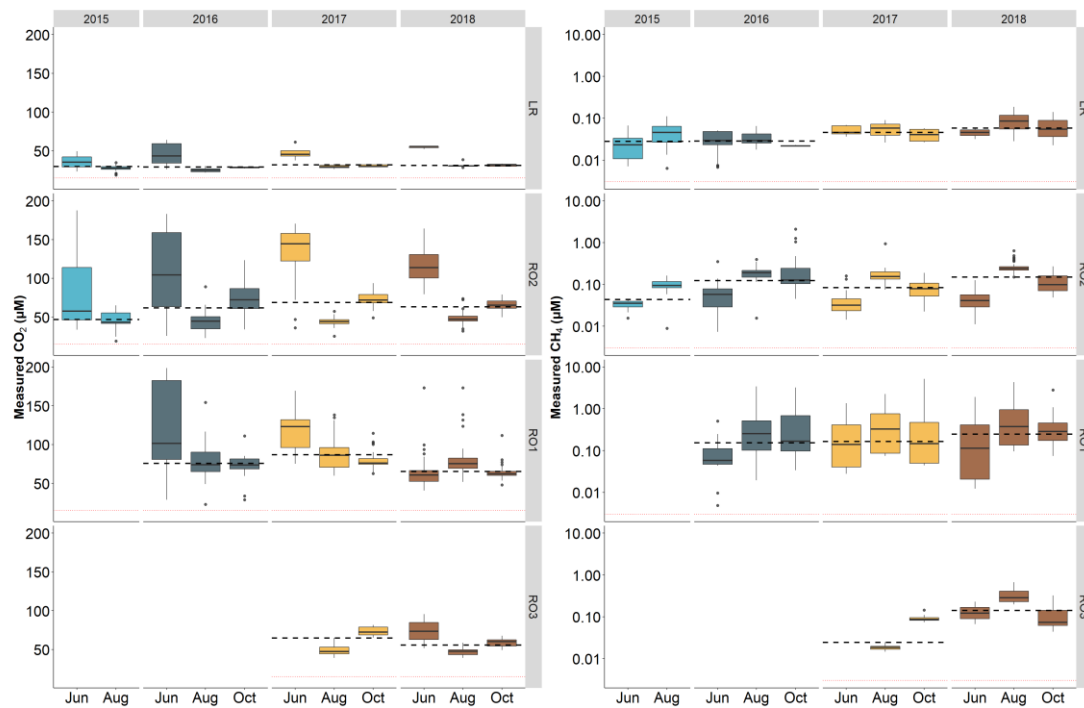


Figure 1.3. Boxplot showing the temporal variability among sampled campaigns, reservoirs, and the La Romaine river (LR) of measured CO_2 (left) and CH_4 (right) concentrations. Boxplots represent median (black line), first and third quartiles (hinges), range (whiskers), and outliers (black dot). The dashed vertical lines represent mean annual concentrations of CO_2 and CH_4 , respectively.

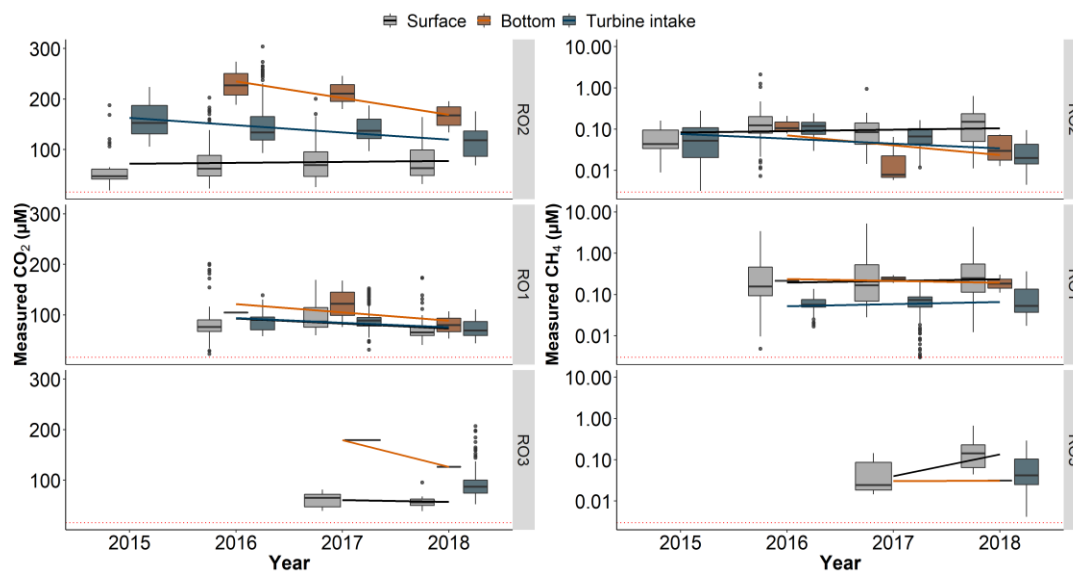


Figure 1.4. Comparison of measured CO_2 (left) and CH_4 concentrations (right) of the surface, bottom and turbine intake of the three studied reservoirs. Boxplots represent median (black line), first and third quartiles (hinges), range (whiskers), and outliers (black dot). Lines represents regressions lines grouped by sampling site depth/location (colors match of the lines match with the colors of the boxplots).

The three reservoirs differed in their average CO_2 and CH_4 concentrations (Figure S1.4). The average CO_2 concentrations over all sampling campaigns in RO3 ($55 \pm 13 \mu\text{M}$) was significantly lower ($p < 0.001$) in comparison with CO_2 concentrations of both RO1 ($81 \pm 23 \mu\text{M}$) and RO2 ($76 \pm 38 \mu\text{M}$). In contrast, average CH_4 concentrations in RO1 ($0.5 \pm 0.7 \mu\text{M}$) were significantly higher ($p < 0.001$) compared to RO2 ($0.14 \pm 0.007 \mu\text{M}$) and RO3 ($0.15 \pm 0.14 \mu\text{M}$). In addition, CO_2 and CH_4 concentrations varied spatially within each reservoir (Figure 1.5). The largest within reservoir CO_2 variability was observed during the spring seasons, ranging from 28 to 200 μM in RO1, 25 to 202 μM in RO2, and 51 to 95 μM in RO3. For CH_4 concentrations, the highest within reservoir spatial variability was observed in the summer, with values ranging from 0.01 to 4.3 μM in RO1, from 0.008 to 0.94 μM in RO2, and from 0.01 to 0.67 μM in RO3. In general, the spatial variability in CO_2 and CH_4 concentrations within reservoirs was related to the sampling location and to the

pre-flood land cover underlying the sampling site. Sampling sites located over wetland and broadleaves forest, or in shallow bays and near to the shore had higher levels of both gases than the main channel of the reservoir (Figure 1.5). In this regard, considering all reservoir data together, the regression tree analysis showed that sampling sites with less than 4.7 meters of depth had higher average CO₂ concentrations (n = 168, mean: 88.9 μM) than deeper sites (n = 570, 73.7 μM, p = 0.04, Figure S1.6). A similar pattern was observed for sampling sites close to the shore (less than 68.9 meters), which had higher average concentrations (n = 276, 83.3 μM) than sites further offshore (n = 462, 73.5 μM, p = 0.02, Figure S1.6). Likewise, the same analysis for CH₄ concentrations also showed that shallower sites (less than 2.7 meters, p < 0.001, Figure S1.6) and sites closer to the shore (less than 30 meters, p < 0.001, Figure S1.6) had higher average CH₄ concentrations (n = 90, 0.98 μM and n = 133, 0.75 μM, respectively) than deeper sites and sites further offshore. The regression tree analysis also showed that sites previously underlain by wetlands had significantly higher CO₂ concentrations than all other sites in RO1 (n = 15, 109 μM, p = 0.004, Figure S1.7; others, n = 293, 80 μM), whereas sites underlain by broadleaves forest, mixed wood and shrub low had significantly higher (p < 0.001, Figure S1.7) CO₂ concentrations (n = 62, 106 μM) than all other sites in RO2 (n = 317, 71 μM); RO3 did not show any dependency on pre-flood land cover. For CH₄, only RO1 reservoir showed dependency on pre-flood land cover, sites previously underlain by wetlands had significantly higher CH₄ concentrations than all other sites (n = 12, 1.7 μM, p = 0.004, Figure S1.7).

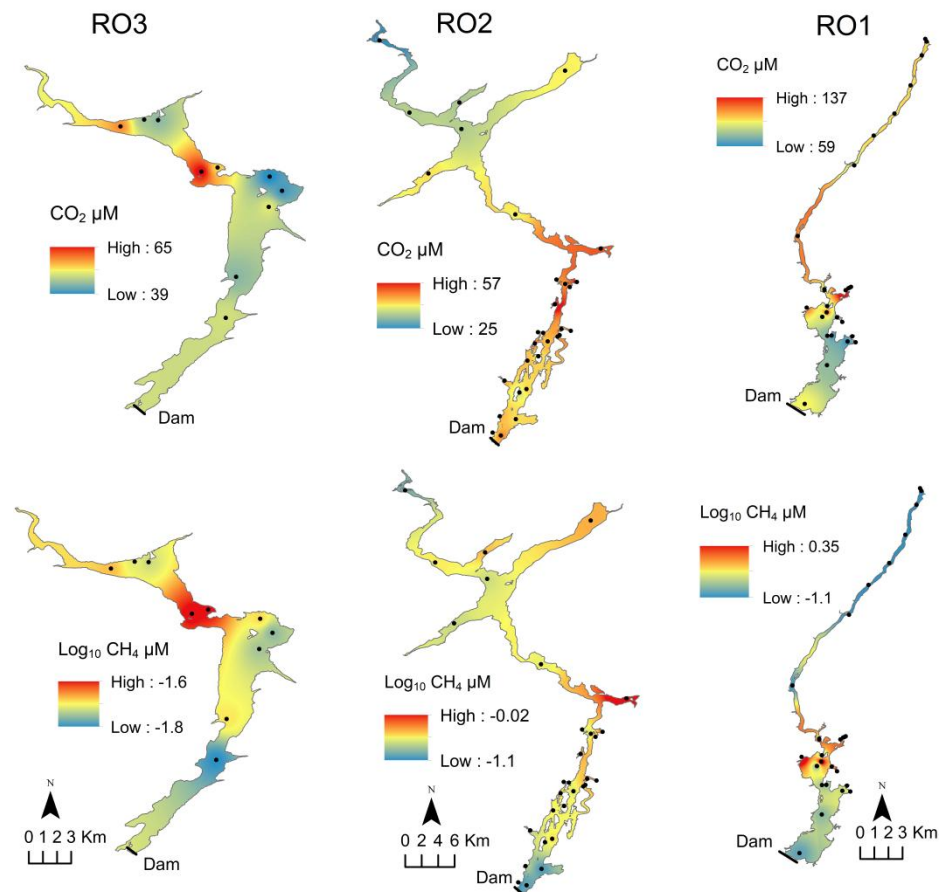


Figure 1.5. Measured CO₂ and CH₄ concentrations from all the three reservoirs in August 2017. Figure is set in order of appearance in the cascade configuration. Each black dot represents a sampling site. The scales of the color bars are different from each other to better visualize spatial variabilities.

1.4.2 Effects of spatial and temporal variables on CO₂ and CH₄ concentrations

Considering the very weak relationship that was observed between the measured CO₂ and CH₄ concentrations (Fig. 1.2), it was necessary to build separate models for the two gases. For both CO₂ and CH₄ the model that combined all three reservoirs resulted in generally weaker model performance ($R^2 = 0.52$ for CO₂ and $R^2 = 0.66$ for CH₄) compared to individual reservoir models (CO₂: R^2 0.59, 0.77, 0.66 for RO1, RO2, RO3, respectively; CH₄: R^2 0.83, 0.64, 0.67 for RO1, RO2, RO3, respectively), and we therefore decided to pursue the latter for all subsequent analyses.

The models for CO₂ differed somewhat between reservoirs, and the selected variables were not always the same, for example site depth was selected in RO1 but not in RO2. Overall, day of the year, water temperature and site depth had a negative effect on CO₂ concentration (Table 1.4). In RO2 the interaction between day of the year and water temperature was more significant than both variables separately ($p = 0.01$). Reservoir age had a negative effect only in RO1, although this effect was barely not significant ($p = 0.06$). Land cover type was selected in RO1 and RO2, in RO1 sites underlain by wetlands had higher CO₂ concentrations, whereas broadleaves forest, mixed wood and shrub pre-flood land covers had a positive effect on CO₂ concentrations in RO2. The selected models for CH₄ were more similar between reservoirs compared to the ones selected for CO₂. We found a positive effect of water temperature and a negative effect of the site depth on the CH₄ concentration in all reservoirs, except in RO1, where the previous underlying land cover ($p < 0.001$) was additionally selected (Table 1.4). The latter occurred due to presence of wetlands that showed a positive effect on CH₄ concentrations.

Table 1.4. Results of linear mixed models, testing effects of the spatial and temporal variables on CO₂ and CH₄ concentrations in each of the three reservoirs. Site ID and sampling campaigns were included as a random effect on the intercept. Significances of fixed effects were assessed with likelihood ratio tests with degrees of freedom = 1. The slope direction (sign) of the effect is indicated with – or +.

Reservoir	Variable	Fixed effect	χ^2	p	*R ²
RO1	CO ₂	– Day of the year	4.6	0.03	
		– Reservoir age	3.4	0.06	
		– Site depth	6.1	0.01	
		± Land cover type	10.2	0.03	0.59
RO2	CO ₂	– Day of the year			
		– Water temperature			
		+ Day of the year × Water temperature	6.4	0.01	
		± Land cover type	10.7	0.09	0.77
RO3	CO ₂	– Water temperature	5.4	0.01	
		– Site Depth	2.3	0.12	0.66
RO1	<i>log</i> ₁₀ CH ₄	+ Water Temp.	12.4	<0.01	
		– Depth	9.5	<0.01	
		± Land cover type	19.7	<0.01	0.83
RO2	<i>log</i> ₁₀ CH ₄	+ Water temperature	6.7	<0.01	
		– Site Depth	10.6	<0.01	0.64
RO3	<i>log</i> ₁₀ CH ₄	+ Water temperature	4.4	0.03	
		– Site Depth	7.3	<0.01	0.67

*Conditional R² considers the variance of both the fixed and random effects.

1.4.3 Temporal and spatial variability of modeled CO₂ and CH₄ concentrations

We used the LMMs in Table 1.4 to reconstruct daily CO₂ and CH₄ concentrations in each of the 30 x 30 m grid cells for the ice-free period, and thus generated a area-wide cartography of gas concentrations for each of the three reservoirs. The modeled CO₂ and CH₄ concentrations varied spatially within each reservoir, and followed a similar spatial pattern as the measured concentrations (Fig. 1.6). Overall, grids located over wetlands, broadleaves forest, mixed wood and shrub, and in shallow areas, had higher levels of both gases than the main channel of the reservoir.

The integrated reservoir CO₂ and CH₄ concentrations, which result from averaging the modeled concentration for all the grid cells within each reservoir, followed a clear seasonal pattern, with high spring CO₂ values and decrease towards the summer, with a subsequent CO₂ build up between summer and autumn in RO2 and RO3, whereas modeled CH₄ concentrations always peaked in the summer in all the three reservoirs, in agreement with our observations (Fig. 1.7). Also, the modeled CO₂ and CH₄ values differed between reservoirs, also in agreement with our measured observations.

Overall, the temporally (seasonal and interannual) and spatially (among and within reservoirs) integrated modeled values followed the same pattern as the measured concentrations, with similar averages (Fig. 1.8). For instance, both average modeled and measured CO₂ values were lower in RO3 ($58 \pm 9 \mu\text{M}$ and $55 \pm 13 \mu\text{M}$, respectively) relative to RO2 ($77 \pm 13 \mu\text{M}$ and $76 \pm 39 \mu\text{M}$, respectively) and RO1 ($78 \pm 17 \mu\text{M}$ and $81 \pm 23 \mu\text{M}$, respectively). Whereas, modeled and measured CH₄ were on average significantly higher ($p = 0.001$) in RO1 ($0.24 \pm 0.14 \mu\text{M}$ and $0.5 \pm 0.75 \mu\text{M}$, respectively) than in RO2 ($0.09 \pm 0.007 \mu\text{M}$ and $0.14 \pm 0.16 \mu\text{M}$, respectively) and RO3 ($0.1 \pm 0.14 \mu\text{M}$ and $0.15 \pm 0.14 \mu\text{M}$, respectively).

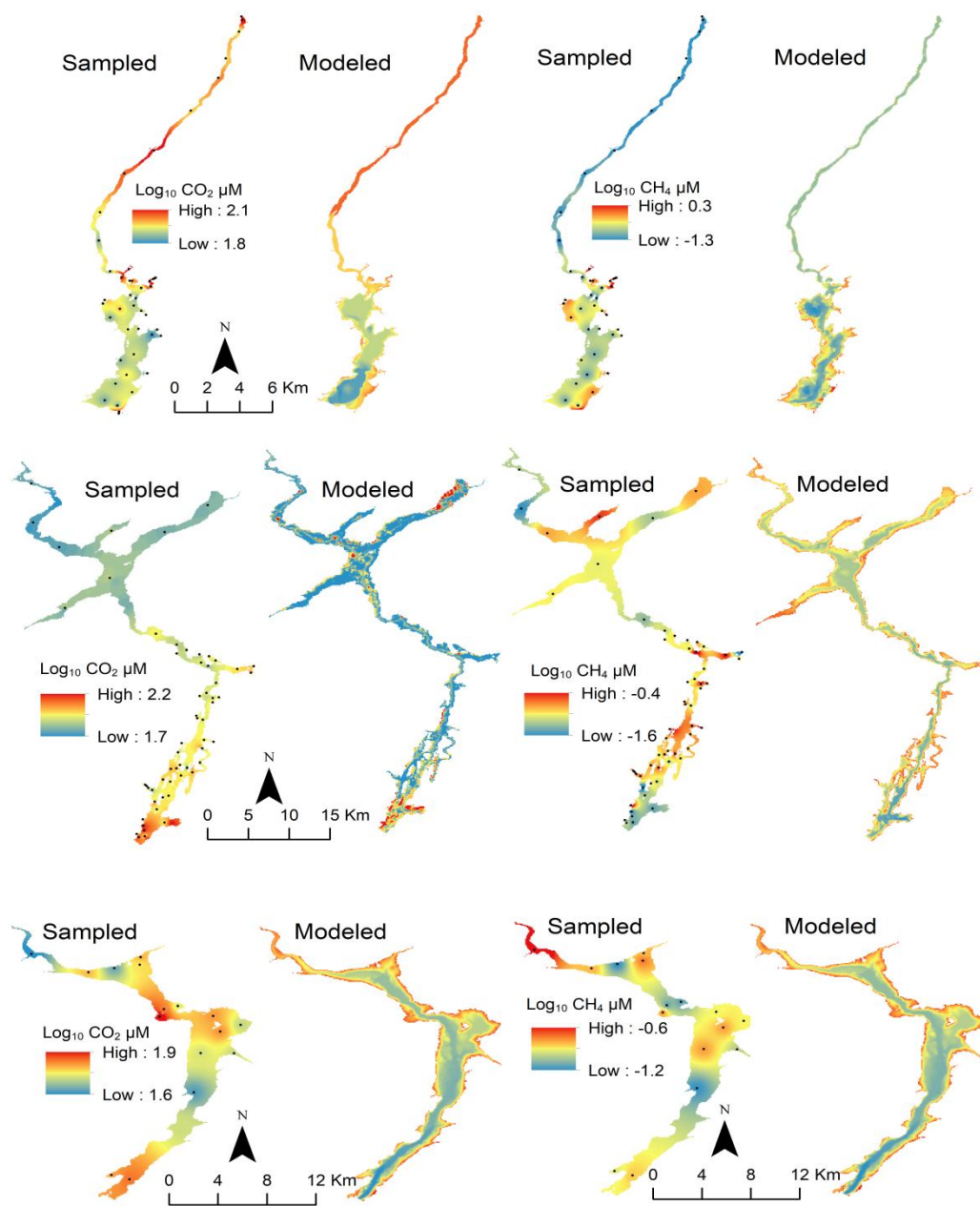


Figure 1.6. Measured and modeled CO_2 and CH_4 concentrations from all the three reservoirs. Each black dot represents a sampling site. The scales of the color bars are different from each other to better visualize spatial variabilities

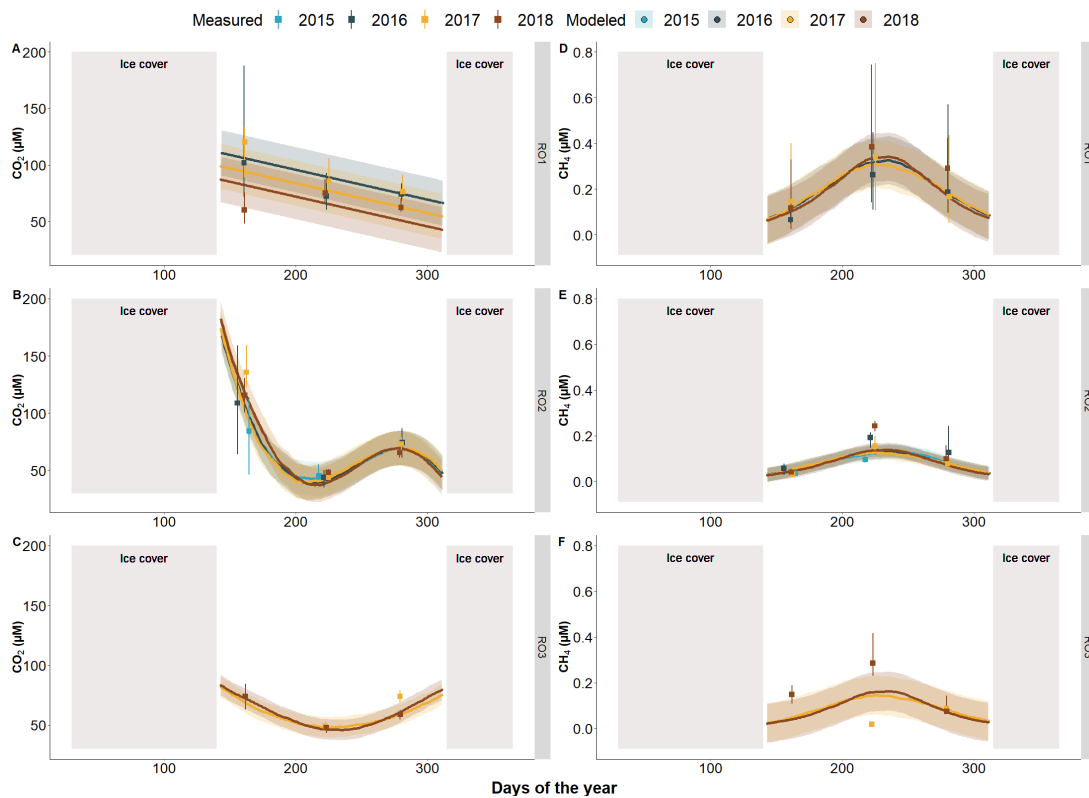


Figure 1.7. Modeled concentrations of CO_2 (left) and CH_4 (right) over individual days in the ice free period. Each dot represents the modeled average of the CO_2 and CH_4 concentration in a day. Shaded polygons around the dots indicate 95% confidence interval for the mean. The square shape and error bars represents the measured CO_2 and CH_4 concentration (median and inter quartile range) of each sampled campaign.

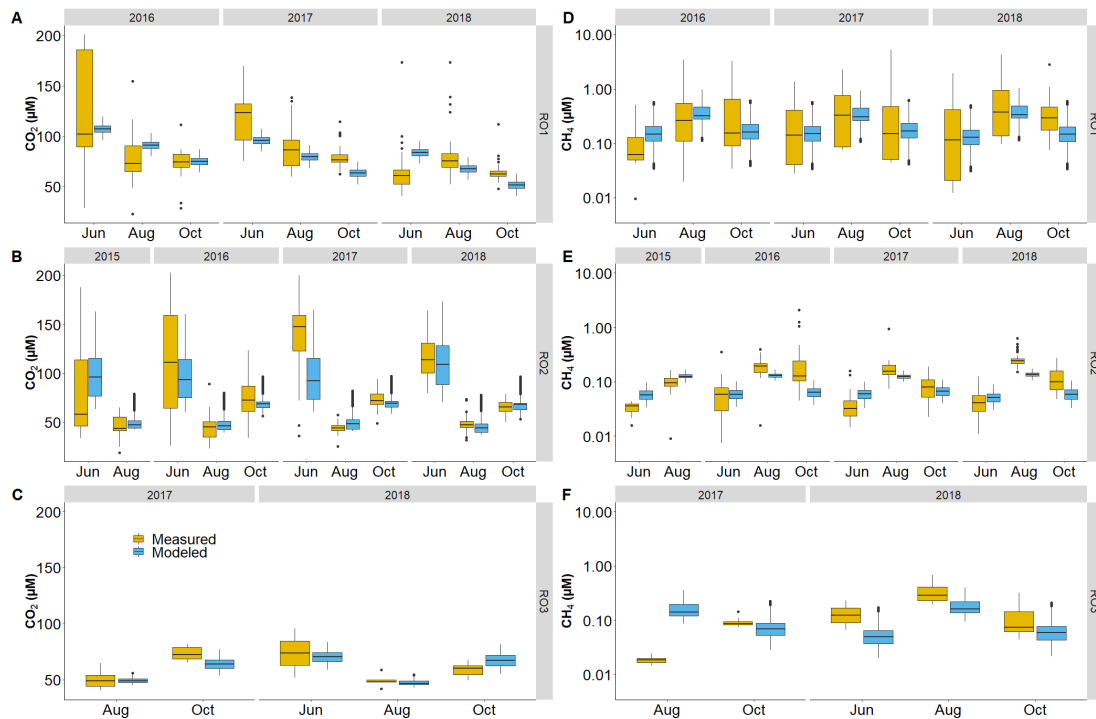


Figure 1.8. Boxplot showing the measured (yellow) and modeled (blue) concentrations of CO₂ and CH₄ (right) over the field campaigns in the ice free period over the years. . Boxplots represent median (black line), first and third quartiles (hinges), range (whiskers), and outliers (black dot).

1.5 Discussion

Despite the growing awareness of hydroelectric reservoirs as greenhouse gases sources to the atmosphere at the global scale (Deemer *et al.*, 2016) and the crucial role of adequate spatial and temporal assessments of CO₂ and CH₄ concentrations and emissions from reservoirs to determine accurate carbon budgets, few studies account and integrate spatially and temporally variability of gas concentrations in these systems (Morales - Pineda *et al.*, 2014; Paranaíba *et al.*, 2018; Roland *et al.*, 2010). To our knowledge, this is the first study that integrates the spatial and temporal variability of both CO₂ and CH₄ concentrations in a cascade hydropower reservoir complex. We observed a large variability in surface water CO₂ and CH₄ concentrations within and among the three studied reservoirs and over seasons, but in contrast to other studies (Abril *et al.*, 2005; Deshmukh *et al.*, 2018), there was not a consistent decrease pattern in surface water gas concentrations over the initial years of flooding. Our modeling exercise of these concentrations reveals that some of the spatial variability may be attributed to the different pre-flooded land cover types, and also to reservoir morphometry, and further that the drivers of CO₂ and CH₄ dynamics in the three reservoirs differ. In this regard, the modeling of spatial and temporal CO₂ and CH₄ concentration provides fundamental insight on the factors underlying C dynamics in these boreal cascade reservoirs. The fact that these models are exclusively based on remotely available variables is particularly useful because they provide effective tools for extrapolation and upscaling of these gas concentrations for the purpose of improving reservoir C footprint estimates.

1.5.1 Temporal and spatial variability of measured CO₂ and CH₄ concentrations

Seasonal variability of measured CO₂ and CH₄ concentrations

The three reservoirs were consistently supersaturated in both CO₂ and CH₄ during the sampled period and hence a constant source of CO₂ and CH₄ to the atmosphere (Figure 1.2), and the range in CO₂ concentrations was in line with previous reports from boreal reservoirs (Demarty *et al.*, 2009; Teodoru, C *et al.*, 2011). We observed clear seasonal patterns in the surface CO₂ concentrations across the studied reservoirs, with highest CO₂ concentrations consistently occurring in spring and likely reflecting CO₂ accumulation under the ice cover during the winter months (Bastien *et al.*, 2011). CO₂ degassing following ice thaw gradually decreased CO₂ concentrations in surface waters, which reached the lowest values during the summer. In the autumn, CO₂ concentrations increased again in the deeper RO2 and RO3 reservoirs (maximum depths 120 m and 90 m, respectively) due to water column turnover and mixing with CO₂-rich hypolimnetic waters (Figure 1.3). In contrast, the shallower RO1 reservoir (maximum depth 30 m) was never fully stratified and did not develop a hypolimnion, and therefore there was no autumn increase in surface CO₂ concentrations but rather a linear decrease in CO₂ concentrations from spring to autumn. These contrasting CO₂ seasonal patterns among reservoirs suggest that CO₂ dynamics are tightly related to reservoir morphometry, and these can differ greatly among reservoirs located close to each other and subjected to the same climate (Figure 1.1).

CH₄ concentrations were in general similar than those reported for others boreal reservoirs. One exception was RO1, where the maximum concentration measured (5.2 µM) was higher than in the Grand Rapids reservoir and in the Eastmain-1 reservoir (1.0 µM, Manitoba, Canada and 0.8 µM, Quebec, Canada, respectively, Demarty *et al.*, 2009). However the CH₄ concentrations median (0.21 µM) in RO1 was similar compared to the CH₄ concentrations median (0.12 µM) from two reservoirs in the boreal zone in Finland (Huttunen *et al.*, 2002). Compared to CO₂, the

CH₄ concentrations showed a more consistent temporal pattern among the reservoirs, with highest CH₄ concentrations consistently observed in the summer campaigns in all the three reservoirs, likely reflecting the strong dependency of CH₄ production on temperature (Yvon-Durocher *et al.*, 2014). In contrast to CO₂, we did not detect high CH₄ concentrations in the spring after the ice melt, or after autumn overturn. Potential explanations are (i) a lack of CH₄ accumulation under the ice due to low production rates during the winter given the strong temperature dependency of CH₄ production on (Bastien *et al.*, 2011), or (ii), a very strong and rapidly CH₄ emissions after the ice cover thaw (Karlsson *et al.*, 2013), due its low solubility in water.

Despite its importance, very few studies have explored the seasonality of both gases concentrations and emissions in reservoirs, particularly in northern landscapes (but see e.g. Bastien *et al.*, 2011, Demarty *et al.*, 2011). Wik *et al.* (2016) suggested that CH₄ emission estimates for northern lakes may be highly biased by short sampling periods, and reported uncertainties of around one order of magnitude associated to temporal overestimates or underestimates in CH₄ emissions. Our results also highlight the importance of sampling all seasons to obtain more accurate estimate of gas concentrations. For example, the CO₂ concentrations would be underestimated by 75% if the sampling campaigns were carried out only during the summer compared to the spring campaigns, whereas the CH₄ concentrations would be 4.5 times larger if the sampling campaigns were carried out only during the summer compared to the spring campaigns. Thus, skipping seasons in the sampling design leads to either an under- or overestimation of the annual reservoir carbon budget depending on the GHG measured. This seasonal decoupling of surface water CO₂ and CH₄ concentrations is paramount to be considered in the sampling design of any future studies.

Inter-annual trend of measured CO₂ and CH₄ concentrations

Previous studies have shown a clear negative relationship between CO₂ concentrations and reservoir age over the initial years after flooding (Abril *et al.*, 2005; Teodoru, C. *et al.*, 2012). For example, Teodoru, C. *et al.* (2012) showed a decrease in surface pCO₂ of almost 40% over the first 3 years after the flooding in a boreal reservoir, and a similar decline was also reported in a tropical reservoir (Abril *et al.*, 2005) and in a subtropical reservoir (Deshmukh *et al.*, 2018). However, this relationship was not consistently found in the reservoirs studied here. RO1, the shallowest reservoir, was the only one which showed a significant decline in surface CO₂ over the first 3 years, the surface CO₂ concentrations in 2016 and 2017 were significantly higher than those found in 2018 (Figure 1.4). In the other two deeper reservoirs, the surface CO₂ concentrations remained roughly consistent over the first 4 years (RO2) and 2 years (RO3) post flooding. Interestingly, CO₂ concentrations within the deep layers in those two reservoirs showed a very different temporal pattern than in their surface layers. The deep samples at the respective dams and the automated system at the generating stations, both drawing water from layers below 40 meters, showed a declining trend in CO₂ concentrations over the years (Figure 1.4), which is in line with the decreasing inter-annual trend observed in other reservoirs (Teodoru, C. *et al.*, 2012; Abril *et al.*, 2005; Deshmukh *et al.*, 2018). The decoupling of surface and bottom layers is clearly linked to the depth of the water column, with reservoirs that showed a declining trend in the surface CO₂ concentrations over the initial years after flooding generally being shallow. For example, the average depth of Nam Theun 2 reservoir (Deshmukh *et al.*, 2018) is 8 m, while the average depth of Petite Saut reservoir (Abril *et al.*, 2005) and Eastmain-1 reservoir (Teodoru, C. *et al.*, 2012) is 11 m, and the RO1 reservoir (this study) is 22 m. On the other hand, the average depth of RO2 and RO3 reservoirs is 61 m and 68 m, respectively. Thus, on one hand, in shallow reservoirs there is a closer contact with the flooded soils and a stronger coupling of surface gas dynamics with the ongoing degradation of the

terrestrial organic matter, with the resulting inter-annual trends of the surface CO₂ concentration. On the other hand, in deeper reservoirs other surface sources and processes, such as lateral inputs from groundwater and tributaries, and pelagic metabolism may influence CO₂ concentrations, and may contribute to the stabilization of the surface concentrations on an inter-annual scale.

The contrasting interannual patterns of surface and deep CO₂ and CH₄ dynamics in surface and bottom waters in these three reservoirs have major implications in the distribution of C emissions in these systems, and how the contribution of the various pathways of emission to the total C footprint will evolve as they evolve in time. Our results suggest that in the deeper reservoirs, the surface diffusive emissions may remain relative constant at least for the initial 4 years post flooding, whereas downstream, emissions through the outlet have likely been declining over this period, whereas in shallow RO1, both surface diffusive and downstream emissions may have been declining over the initial post-flood years.

Regarding the inter-annual variability of CH₄ concentrations, previous studies have shown an initial increase in the first years after flooding, followed by a decline (Abril *et al.*, 2005; Venkiteswaran *et al.*, 2013). The CH₄ concentrations in the water column of a tropical reservoir peaked 1 year after the reservoir flooding and declined in subsequent years (Abril *et al.*, 2005), whereas CH₄ concentrations increased through the first 3 years and declined slightly in the fourth and fifth year in small boreal reservoirs (Venkiteswaran *et al.*, 2013). In the studied reservoirs, we found slightly lower concentrations values in the first year after the reservoirs were flooded and quite stable over the following years (Figure 1.4). This time lag in CH₄ concentration in the reservoirs may be linked to the slow development of anoxic bottom layers in these cold, boreal reservoirs, and the exogenous availability of alternative electron acceptors and labile OM, since the biogenic CH₄ is produced during the final step of anaerobic organic matter degradation when all other inorganic

oxidants such as sulfate or ferric iron were already depleted (Conrad, 2009; Thauer *et al.*, 2008).

Within reservoir spatial variability of measured CO₂ and CH₄ concentrations

Several studies have recently highlighted the high degree of spatial variability of CO₂ and CH₄ concentrations that occurs within reservoirs. For example, shallow and riverine inflow areas are likely to have higher pCO₂ and pCH₄ than the reservoir main channel close to the dam (Paranaíba *et al.*, 2018). Our results based on regression trees analysis showed that reservoir CO₂ and CH₄ concentrations were related to the geographic location of the sampling sites (Figure 1.5, Figure S1.6 and Figure S1.7). Sampling sites located over (i) specific pre-flooded land covers, and (ii) in shallow areas had higher concentrations of both gases than the main channel of the reservoir. In particular, wetland, shrub, mixed wood and broadleaf forests showed higher gas concentrations in surface waters than those overlying coniferous forest, which is potentially due to different organic matter content and composition of each flooded landscape. It has been previously shown that pre-flooded land type influenced post-flood surface water CO₂ dynamics in a boreal reservoir (Soren M. *et al.*, 2012; Teodoru, C *et al.*, 2011), and therefore, a portion of the spatial variability observed can be linked to the pre-flood landscape and its influences, which may conceivably last for several years after flooding. Moreover, we observed higher levels of gases in shallower sites, thus water column depth can also be linked to the gas concentration spatial heterogeneity. As in our study, site depth has been linked to the spatial variation in pCO₂ in a tropical reservoir, where pCO₂ was higher in the shallower sites compared to deeper ones (Roland *et al.*, 2010). Site depth could be a proxy to areas with contact to sediment metabolism, and also higher sedimentation rates, which could lead to higher CO₂ and CH₄ concentrations due to sediment organic matter degradation (Loken *et al.*, 2019; Sobek *et al.*, 2012).

Among reservoir spatial variability of measured surface CO₂ and CH₄ concentrations

Although reservoirs are often built in a cascade configuration along river corridors, only few studies have assessed the inter-spatial variability among reservoirs within a reservoir cascade configuration (Liu *et al.*, 2020; Okuku *et al.*, 2019; Shi *et al.*, 2017). In a reservoir cascade in China (Mekong River), the first two reservoirs (Gongguoqiao and Miaowei reservoirs) were found to be a hotspot of both CO₂ and CH₄ dissolved concentrations and diffusive emissions compared to downstream reservoirs (Liu *et al.*, 2020; Shi *et al.*, 2017), which was linked it to the higher sediment trapping that provided fresh organic carbon to the first reservoirs for mineralization. Previous studies also suggested a link of organic-rich sediment deposition on CH₄ production in reservoirs (Beaulieu *et al.*, 2016; Maeck *et al.*, 2013). Although we have not measured sedimentation in our study, La Romaine is a sediment-poor river, thus we did not observe this link between the gas concentrations and highest sediment trapping in upstream reservoirs. Rather, we attribute the average differences among reservoirs to the pre-flooding land cover and reservoir morphometry. We found CO₂ concentrations were significantly higher in RO2 and RO1 (second reservoir and last in the cascade, respectively), while CH₄ concentrations were clearly highest in RO1 (last reservoir in the cascade). Thus, CO₂ concentrations were significantly higher in RO1 and RO2 where a large portion of the flooded area were composed by wetland, shrub, mixed wood and broadleaf forests (32% and 20% in total, respectively), whereas these land types represent only a small portion of the flooded area in RO3 (4%; Table 1.2). Similarly, CH₄ concentrations were higher in RO1 than in the other reservoirs, reflecting the 4 to 6-fold greater proportion of shrub and wetland flooded areas in RO1 than in RO2 and RO3 reservoirs, respectively (Table 1.2). As mentioned before, such land covers showed higher levels of CO₂ and CH₄ compared to coniferous forest, which covered a larger area in the RO2 and RO3 reservoirs (Table 1.2). In addition, RO1 has a lower mean depth than RO2 and RO3 (Table 1.2), which likely contributes to explaining the

higher observed CH₄ concentrations. Shallow water columns reduce the extent of stratification and increase the connectivity between sediments and surface waters, and therefore the movement of CH₄ from anoxic sediments environment to surface waters.

1.5.2 Modeled CO₂ and CH₄ concentrations with remote available variables: effects and predictions

Although subject to a similar climate, and in close proximity to each other, we found differences in terms of drivers for the three investigated reservoirs. The mixed effect models allowed us to identify the main temporal and spatial variables driving surface water CO₂ and CH₄ concentrations in the individual reservoirs. Temporal variables such as (i) water temperature and (ii) day of the year were utilized to predict the gas concentrations seasonal pattern. Water temperature had a negative effect on CO₂ concentrations in RO2 and RO3 despite the positive dependence of heterotrophic respiration on water temperature (Sand-Jensen *et al.*, 2007; Yvon-Durocher *et al.*, 2014). CO₂ concentrations were higher in June (spring) and October (autumn) when temperatures are much lower compared to August (summer). This relationship does not reflect metabolism, but rather patterns in CO₂ accumulation within the system. Thus, in June, CO₂ concentrations were likely driven by CO₂ accumulation under ice and subsequent thawing rather than due to increased microbial metabolic activity. In October, CO₂ concentrations were likely driven by CO₂ input from the hypolimnion, since RO2 and RO3 presented a stratified water column (Figure 1.4). Similarly, the day of the year in which the samples were taken also had negative effect CO₂ concentrations, but only at RO1 and RO2. Likewise the water temperature, the day of the year seems to be a proxy for the higher CO₂ input from ice cover and snow thaw during June. Thus, our results show that seasonal variability of CO₂ concentrations in boreal reservoir seems to be tightly coupled to the ice regime within the reservoir and surrounding catchment and the reservoirs' morphometry, which controls the water column stratification. In contrast, water temperature had positive effect on CH₄ concentrations in all three reservoirs, showing the expected relationship between CH₄

production and temperature (Yvon-Durocher *et al.*, 2014) and in agreement with our higher CH₄ concentrations measurements in August (summer), the warmest month. Our findings underline the importance of water temperature in predicting the variability of surface water CH₄ concentrations in reservoirs, for instance reservoirs located in tropical regions tropical reservoirs were already linked to higher levels of CH₄ emissions (Barros *et al.*, 2011).

Spatially, site depth and pre-flooded land cover were the strongest predictor variables to model the spatial patterns in gas concentrations. For example, depth and pre-flooded land cover had an effect on CO₂ concentrations in RO1, this may reflect several processes. On one hand, higher concentrations were observed in the shallow channel (average depth of 3.5 m) that connects RO2 to RO1 and RO1 receives CO₂-rich hypolimnion water from RO2. However, this CO₂ is basically all degassed before reaching the lacustrine zone of RO1. On the other hand, highest concentrations were found over shrub, mixedwood forest and wetlands land covers, which were also relatively shallow areas (average depth of 4.8 m). In contrast, site depth was not select in RO2, and only land cover had a significant (negative) effect on CO₂ in this reservoir. Highest CO₂ values were found in the two specific land covers, mixedwood forest and shrub, which are found further south of the reservoir, near the dam. This area is particularly deep, thus the general negative effect of water column depth on CO₂ was not observed in RO2. In contrast, site depth had a negative relationship with CH₄ concentrations in all the three reservoirs. Also, in RO1, land cover had a strong influence in the CH₄ concentrations. In particular, sites overlying wetland and shrub land types had 2 to 5 times higher CH₄ concentrations than other land covers, highlighting the importance of the pre-flood physiognomy on the C dynamics of the reservoir.

Futhermore, if we compare the average of measured values and the average of temporally and spatially-integrated modeled values, they are similar (Figure 1.8).

This happened because our sampling strategy adequately covered different scenarios over time and space. For instance, if we had sampled sites only in the main channel of the reservoirs, the average measured values would be 10% and 40% lower for CO₂ CH₄, respectively than the average of the spatially-integrated modeled values (details not shown). Moreover, the development of temporally and spatially-integrated models allowed us to predict well the concentration of gases in unsampled areas and times under similar conditions. For example, detailed maps (30 m by 30 m) of maximum depth, land cover, and distance from shore allowed us to extrapolate concentrations for similar locations where we did not sample (Figure 1.6). Likewise, the use of temporal variables such as water temperature, allowed us to extrapolate the concentrations for periods between field campaigns (Figure 1.7). Therefore, our spatial and temporal modeling approach used here will allow us to overlay k and extrapolate the emission without time and location bias, which will consequently lead to more reliable emission estimates.

1.5.3 Implications of performed modeling approach

Although hydroelectric reservoir GHG emissions are often highly variable in both space and time (Deemer *et al.*, 2016), some of this temporal and spatial variability can actually follow a pattern and be related to either internal or external drivers. Previous studies have suggested that reservoir age and latitude as significant predictors of both CO₂ and CH₄ emissions (Barros *et al.*, 2011; St Louis *et al.*, 2000). Recently, other studies have associated reservoir size and trophic state to the GHG emissions (Deemer *et al.*, 2016; DelSontro *et al.*, 2018). Here, we utilized temporal and spatial remote available variables (Table 1.3) and developed spatial and temporal integrated empirical models to predict CO₂ and CH₄ concentrations in three reservoirs along a cascade configuration, which were predicted with a resolution of 30 meters and daily. The mixed effect models reproduced the seasonal pattern of CO₂ and CH₄ concentrations relatively well (Figure 1.7), and effectively predicted the increase in

CO₂ concentrations in autumn in RO2 and RO3 due to the water column overturn (Fig. 1.7). The models captured the spatial variability in CO₂ and CH₄ as well, and identified temperature, depth, and pre-flood landcover as key drivers (Figure 1.6). Although CO₂ and CH₄ concentrations are not a direct measure of emissions, they are the most important factor influencing the heterogeneity of these emissions (Morales - Pineda *et al.*, 2014; Paranaíba *et al.*, 2018; Sobek *et al.*, 2005), and therefore understating gas concentrations dynamics is key to effectively modeling diffusive reservoir emissions. Therefore, by using remotely available variables in our model approach, we could not only accurately predict both temporal and spatial gas dynamics in the studied reservoirs, but also improve our understanding of how seasonal, pre-flood land cover and reservoir morphometry characteristics affect C processing in these environments.

1.6 Conclusion

Overall, our results showed that the measured surface CO₂ and CH₄ concentrations were highly variable. Despite that, they followed consistent pattern within the three studied reservoirs and over seasons. This enabled us to develop empirical models using variables that can be accessed remotely. The models explained between 59% to 83% of the variability and revealed that some of the seasonal and spatial heterogeneity can be attributed to specific variables. However, we found differences in terms of drivers for the CO₂ and CH₄ dynamics and for three investigated reservoirs, although they are subject to a similar climate, and in close proximity to each other. Overall, our results showed that spatial variability was linked to the different pre-flooded land cover types, and also to reservoir morphometry. While the seasonal variability of CO₂ concentrations seemed to be coupled to the ice regime within the reservoir and surrounding catchment, the seasonal variability of CH₄ were related positively with warmer water temperatures. Moreover, there was not a

consistent decrease pattern in surface water gas concentrations over the initial years of flooding. But, water from layers below 40 meters showed a declining trend in CO₂ concentrations over the years (Figure 1.4), suggesting that CO₂ concentrations within the deep layers of deep reservoirs follow a different inter-annual pattern than in their surface layers. It is important to acknowledge that the equations showed on table 1.4 are site specific and may not be fully applicable to other situations. Nonetheless, the modeling framework shown here can certainly be applied elsewhere. Finally, combined with appropriate modeled gas transfer models, we expect that our modeled CO₂ and CH₄ concentrations in these newly created hydroelectric complex will eventually increase our overall understanding of the drivers of both spatial and temporal dynamics of these gases in these major boreal reservoirs yielding more accurate and representative estimates of diffusive C emissions from these systems.

ANNEXE A

SUPPORT INFORMATION

Limnological Parameters

All three reservoirs were very similar regarding their limnological characteristics (Table S1.1). The measured average water temperature ranged from 11.4 ± 0.7 °C (mean \pm SD) in RO-1 to 14.7 ± 1.6 °C (mean \pm SD) in RO-3. The pH was slightly acidic with the average ranging from 5.7 in RO-3 to 6.0 in RO-1 and RO-2. The DOC concentration ranged between 4.6 mg L^{-1} in RO-3 and 15 mg L^{-1} in RO-1 (mean $6.0 \pm 2.6 \text{ mg L}^{-1}$), while average DIC concentration ranged from $1.2 \pm 2.6 \text{ mg L}^{-1}$ in RO-3 to $1.5 \pm 2.6 \text{ mg L}^{-1}$ in RO-3. The surface water of all reservoirs was well oxygenated; the averaged oxygen saturation was 92.9 ± 9 % (mean \pm SD) mg L^{-1} . All three reservoirs showed oligotrophic conditions, concentrations of chlorophyll *a* (*Chla*), total phosphorus (TP) and TN (total nitrogen) were low, $1.0 \pm 0.7 \text{ }\mu\text{g/L}$, $10.2 \pm 3.1 \text{ }\mu\text{g/L}$ and $18 \pm 4.2 \text{ }\mu\text{g/L}$ respectively.

Code and data availability: <https://figshare.com/s/bb2f9b80cf31d0bbe9ae>

Table S1.1. Limnological characteristics of the three investigated reservoirs. Average wind speed was measured at 1 m.

	Reservoirs (n = 794)								
	La Romaine 1			La Romaine 2			La Romaine 3		
	Mean (± SD)	Min	Max	Mean (± SD)	Min	Max	Mean (±SD)	Min	Max
DOC (mg/L)	6.2 (± 1.5)	5.2	15.0	5.8 (± 0.5)	4.7	8.0	5.7 (± 0.6)	4.6	6.5
DIC (mg/L)	1.5 (± 0.4)	0.5	3.0	1.4 (± 0.5)	0.7	3.6	1.2 (± 0.1)	0.9	1.3
pH	6.0 (± 0.3)	4.4	6.8	6.0 (± 0.3)	4.6	7.5	5.7 (± 0.3)	5.2	6.3
OD (%)	92.5 (± 8.9)	59.2	113.6	91.9 (± 12)	14.2	114.9	94.3 (± 6.2)	118	83.7
<i>Chla</i> (µg/L)	1.1 (± 0.9)	0	5.9	1.0 (± 0.8)	0	6.4	0.2 (± 0.4)	0	0.5
TP (µg/L)	11.2 (± 3.6)	5.7	32	9.4 (± 4.5)	3.7	57.2	9.0 (± 1.6)	6.4	12.3
TN (mg/L)	0.19 (± 0.07)	0.04	0.45	0.17 (± 0.05)	0.03	0.37	0.16 (± 0.01)	0.1	0.2
Water Temp.(°C)	11.4 (± 4.1)	3.6	19.8	13.0 (± 5.9)	3.1	23.6	14.7 (± 5.1)	5.3	22.0
Average Wind speed (m/s)	2.8 (± 1.6)	0	9.6	2.3 (± 1.5)	0	8.2	2.6 (± 1.8)	0.2	6.8

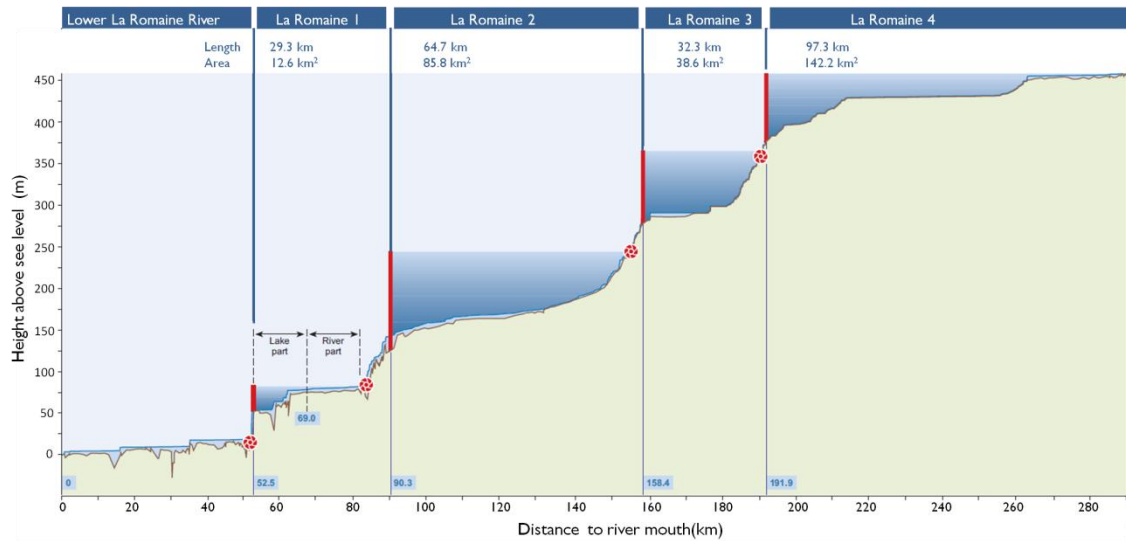


Figure S1.1. Figure showing the cascade reservoir configuration in the La Romaine river.

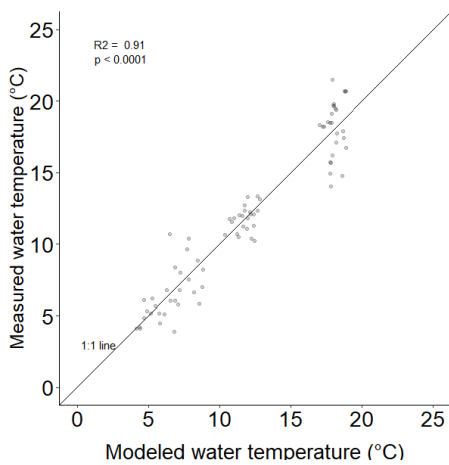


Figure S1.2. Relationship between measured and modeled water temperature

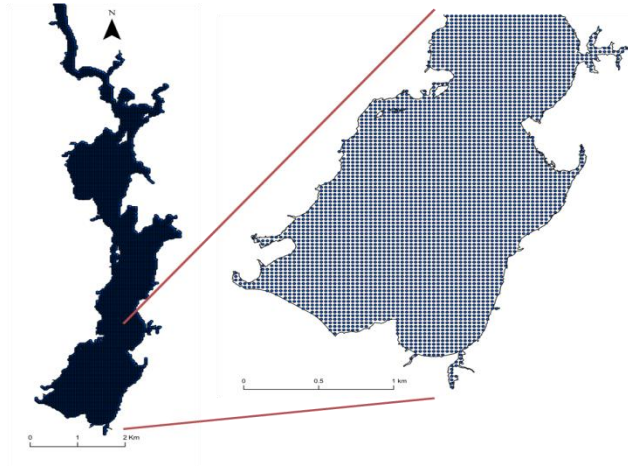


Figure S1.3. Map of the La Romaine I dam showing the grid points (30 m x 30m) generated using the fishnet toolbox in ArcMap 10.

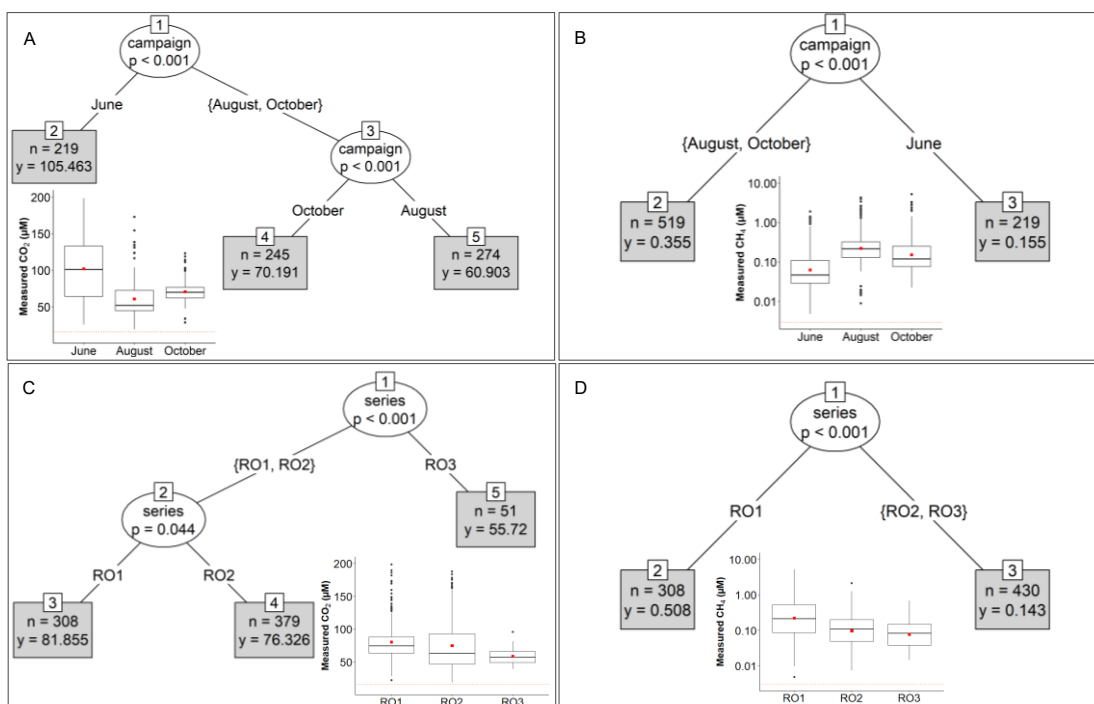


Figure S1.4. Regression tree showing the variability among seasons and reservoirs of CO_2 (A and C) and CH_4 (C e D) concentrations.

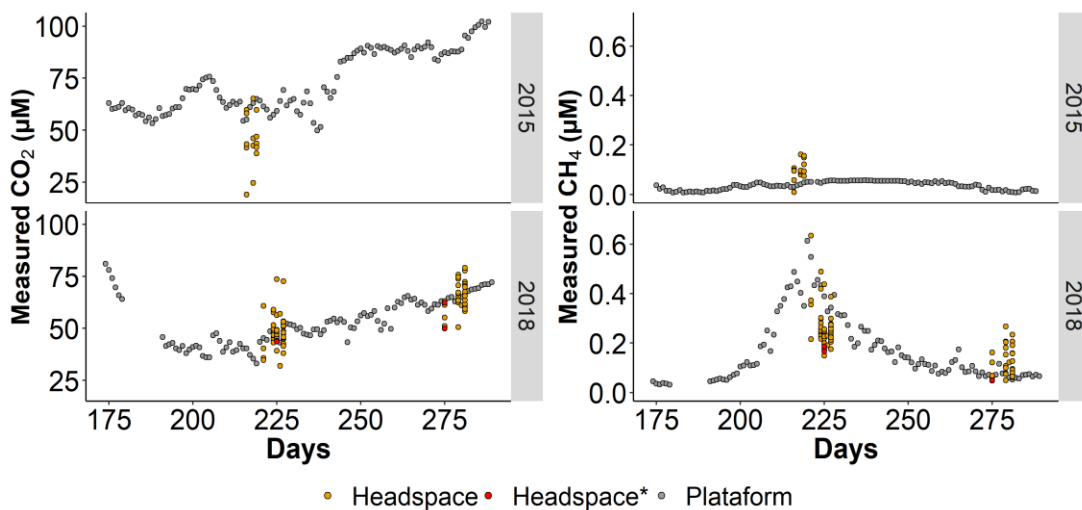


Figure S1.5. Scatterplot showing the daily average of CO₂ and CH₄ of the platform (grey dots) and our sampling sites (yellow dots and red dots). *Sample location next to the platform.

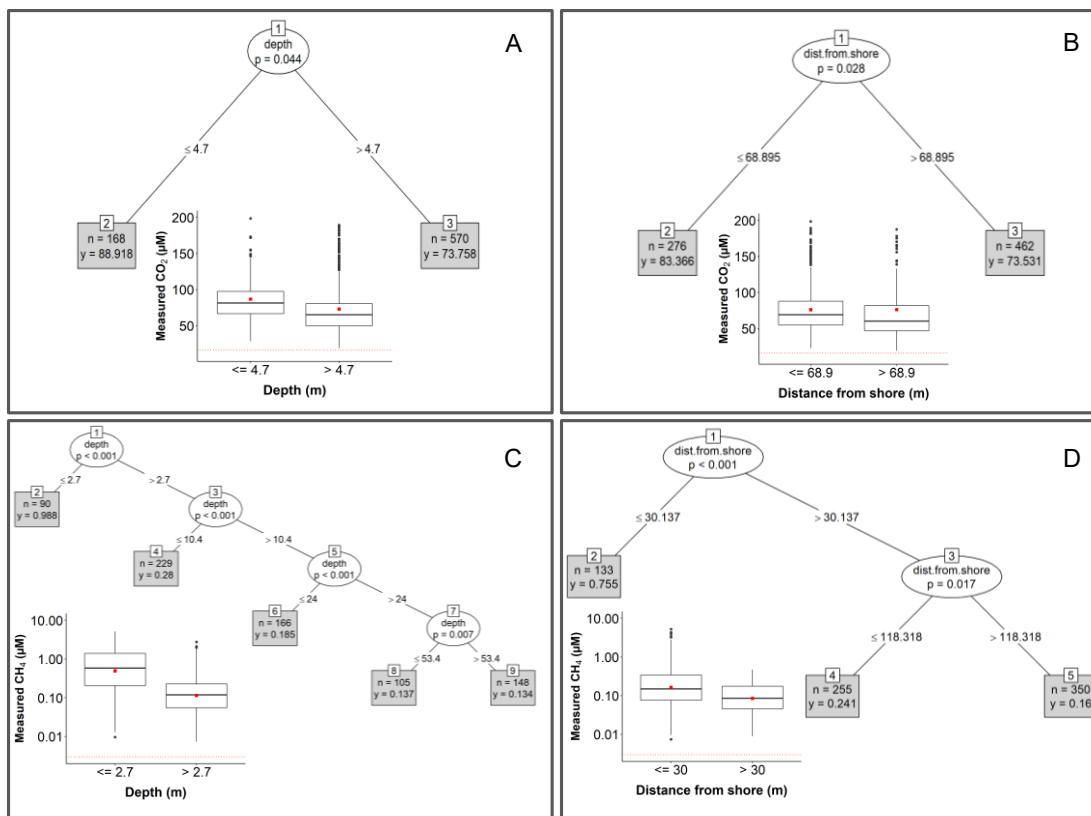


Figure S1.6. Regression tree showing the relationship of depth and distance from shore of CO_2 (A and B) and CH_4 (C e D) concentrations.

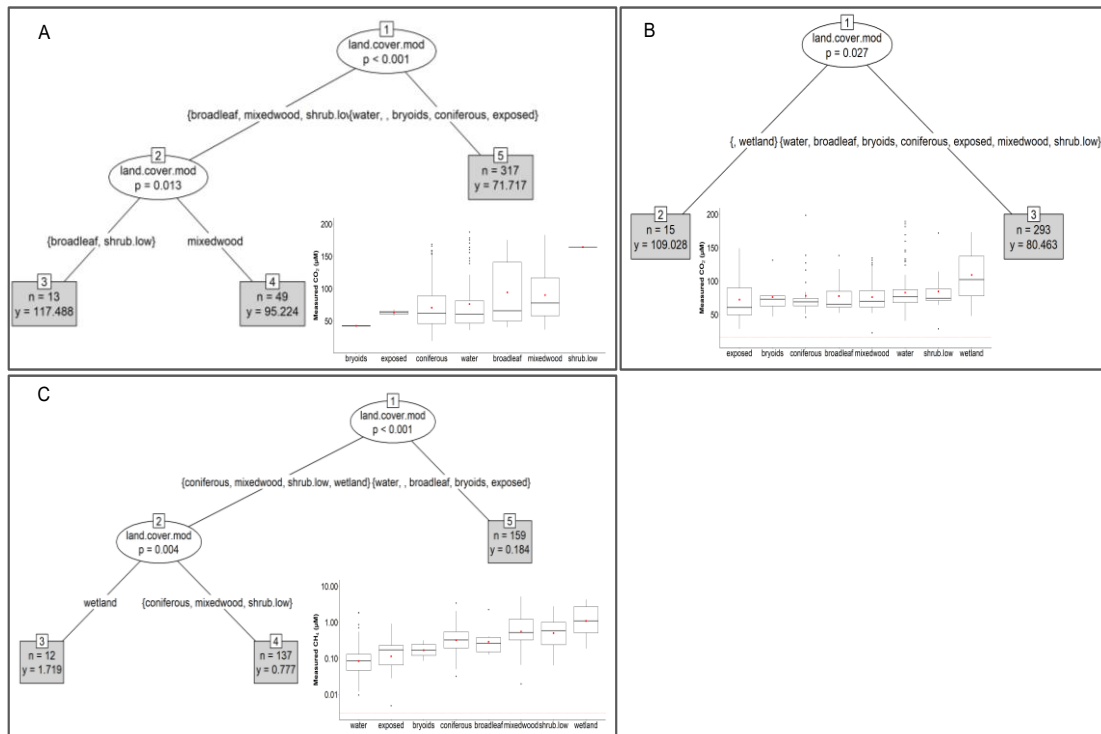


Figure S1.7 Rregression tree showing the relationship between the underlain land cover and CO₂ concentrations in RO2 (A) and CH₄ and CO₂ concentrations (B e C, respectively) in RO1 .

RÉFÉRENCES

- Abe, D. S., Adams, D. D., Galli Corina, V. S., Sikar, E. et Tundisi, J. G. (2005). Sediment greenhouse gases (methane and carbon dioxide) in the Lobo - Broa Reservoir, São Paulo State, Brazil: Concentrations and diffuse emission fluxes for carbon budget considerations. *Lakes & Reservoirs: Science, Policy and Management for Sustainable Use*, 10(4), 201-209. doi: doi:10.1111/j.1440-1770.2005.00277.x
- Abril, G., Guerin, F., Richard, S., Delmas, R., Galy-Lacaux, C., Gosse, P., . . . Matvienko, B. (2005, Oct 13). Carbon dioxide and methane emissions and the carbon budget of a 10-year old tropical reservoir (Petit Saut, French Guiana). *Global Biogeochemical Cycles*, 19(4). doi: Artn Gb4007 Doi 10.1029/2005gb002457
- Abril, G., Martinez, J. M., Artigas, L. F., Moreira-Turcq, P., Benedetti, M. F., Vidal, L., . . . Roland, F. (2014, Jan 16). Amazon River carbon dioxide outgassing fuelled by wetlands. *Nature*, 505(7483), 395-+.
- Aufdenkampe, A. K., Mayorga, E., Raymond, P. A., Melack, J. M., Doney, S. C., Alin, S. R., . . . Yoo, K. (2011, Feb). Riverine coupling of biogeochemical cycles between land, oceans, and atmosphere. *Frontiers in Ecology and the Environment*, 9(1), 53-60. doi: Doi 10.1890/100014
- Barros, N., Cole, J. J., Tranvik, L. J., Prairie, Y. T., Bastviken, D., Huszar, V. L. M., . . . Roland, F. (2011, Sep). Carbon emission from hydroelectric reservoirs linked to reservoir age and latitude. *Nature Geoscience*, 4(9), 593-596. doi: Doi 10.1038/Ngeo1211
- Bastien, J., Demarty, M. et Tremblay, A. (2011, 2011/01/01). CO₂ and CH₄ diffusive and degassing emissions from 2003 to 2009 at Eastmain 1 hydroelectric reservoir, Québec, Canada. *Inland Waters*, 1(2), 113-123. doi: 10.5268/IW-1.2.349

- Bastien, J., Demarty, M., Tremblay, A. et Gill, R. (2009, 01/01). Use of automated systems to measure greenhouse gas emissions from reservoirs. *Air and Waste Management Association - 1st International Greenhouse Gas Measurement Symposium 2009*, 182, 154-159.
- Bastviken, D., Cole, J., Pace, M. et Tranvik, L. (2004, Oct 20). Methane emissions from lakes: Dependence of lake characteristics, two regional assessments, and a global estimate. *Global Biogeochemical Cycles*, 18(4).
- Bastviken, D., Tranvik, L. J., Downing, J. A., Crill, P. M. et Enrich-Prast, A. (2011, Jan 7). Freshwater methane emissions offset the continental carbon sink. *Science*, 331(6013), 50. doi: 10.1126/science.1196808
- Bates, D., Mächler, M., Bolker, B. et Walker, S. (2015, 2015-10-07). Fitting Linear Mixed-Effects Models Using lme4. 2015, 67(1), 48. doi: 10.18637/jss.v067.i01
- Beaulieu, J. J., McManus, M. G. et Nietch, C. T. (2016). Estimates of reservoir methane emissions based on a spatially balanced probabilistic - survey. *Limnology and Oceanography*, 61(S1), S27-S40.
- Benoit, T. et Achraf, E. (2019). Package 'suncalc' version 0.5.
- Bolker, B. M. (2015). Linear and generalized linear mixed models. *Ecological Statistics: Contemporary theory and application*, 309-333.
- Chao, B. F., Wu, Y. H. et Li, Y. S. (2008). Impact of Artificial Reservoir Water Impoundment on Global Sea Level. *Science*, 320(5873), 212-214. doi: 10.1126/science.1154580
- Chowdhury, T. R. et Dick, R. P. (2013). Ecology of aerobic methanotrophs in controlling methane fluxes from wetlands. *Applied Soil Ecology*, 65, 8-22.
- Cole, J. J. et Caraco, N. F. (1998, Jun). Atmospheric exchange of carbon dioxide in a low-wind oligotrophic lake measured by the addition of SF₆. *Limnology and Oceanography*, 43(4), 647-656.

- Cole, J. J., Prairie, Y. T., Caraco, N. F., McDowell, W. H., Tranvik, L. J., Striegl, R. G., . . . Melack, J. (2007, Feb). Plumbing the global carbon cycle: Integrating inland waters into the terrestrial carbon budget. *Ecosystems*, *10*(1), 171-184. doi: DOI 10.1007/s10021-006-9013-8
- Conrad, R. (2009). The global methane cycle: recent advances in understanding the microbial processes involved. *Environmental Microbiology Reports*, *1*(5), 285-292. doi: 10.1111/j.1758-2229.2009.00038.x
- Deemer, B. R., Harrison, J. A., Li, S., Beaulieu, J. J., DelSontro, T., Barros, N., . . . Vonk, J. A. (2016). Greenhouse Gas Emissions from Reservoir Water Surfaces: A New Global Synthesis. *BioScience*, *66*(11), 949-964. doi: 10.1093/biosci/biw117
- DelSontro, Beaulieu, J. J. et Downing, J. A. (2018). Greenhouse gas emissions from lakes and impoundments: Upscaling in the face of global change. *Limnology and Oceanography Letters*, *3*(3), 64-75.
- Delsontro, T., McGinnis, D. F., Sobek, S., Ostrovsky, I. et Wehrli, B. (2010, Apr 1). Extreme Methane Emissions from a Swiss Hydropower Reservoir: Contribution from Bubbling Sediments. *Environmental Science & Technology*, *44*(7), 2419-2425. doi: Doi 10.1021/Es9031369
- Demarty, M., Bastien, J. et Tremblay, A. (2011). Annual follow-up of gross diffusive carbon dioxide and methane emissions from a boreal reservoir and two nearby lakes in Québec, Canada. *Biogeosciences*, *8*(1).
- Demarty, M., Bastien, J., Tremblay, A., Hesslein, R. H. et Gill, R. (2009, 2009/12/01). Greenhouse Gas Emissions from Boreal Reservoirs in Manitoba and Québec, Canada, Measured with Automated Systems. *Environmental Science & Technology*, *43*(23), 8908-8915. doi: 10.1021/es8035658
- Denfeld, B. A., Lupon, A., Sponseller, R. A., Laudon, H. et Karlsson, J. (2020, 2020/07/02). Heterogeneous CO₂ and CH₄ patterns across space and time in a small boreal lake. *Inland Waters*, *10*(3), 348-359. doi: 10.1080/20442041.2020.1787765
- Deshmukh, C., Guérin, F., Vongkhamsoo, A., Pighini, S., Oudone, P., Sopraseuth, S., . . . Oliva, P. (2018). Carbon dioxide emissions from the flat bottom and

shallow Nam Theun 2 Reservoir: drawdown area as a neglected pathway to the atmosphere. *Biogeosciences*, 15(6), 1775-1794.

dos Santos, M. A., Damázio, J. M., Rogério, J. P., Amorim, M. A., Medeiros, A. M., Abreu, J. L. S., . . . Rosa, L. P. (2017, 2017/08/15/). Estimates of GHG emissions by hydroelectric reservoirs: The Brazilian case. *Energy*, 133, 99-107. doi: <https://doi.org/10.1016/j.energy.2017.05.082>

Downing, J. A., Prairie, Y. T., Cole, J. J., Duarte, C. M., Tranvik, L. J., Striegl, R. G., . . . Middelburg, J. J. (2006). The global abundance and size distribution of lakes, ponds, and impoundments. *Limnology and Oceanography*, 51(5), 2388-2397. doi: 10.4319/lo.2006.51.5.2388

Duchemin, E., Lucotte, M., Canuel, R. et Chamberland, A. (1995). Production of the greenhouse gases CH₄ and CO₂ by hydroelectric reservoirs of the boreal region. *Global Biogeochemical Cycles*, 9(4), 529-540.

Fearnside, P. M. (2001). Environmental impacts of Brazil's Tucuruí Dam: Unlearned lessons for hydroelectric development in Amazonia. *Environmental management*, 27(3), 377-396.

Fearnside, P. M. (2006, Mar). Greenhouse gas emissions from hydroelectric dams: Reply to Rosa et al. *Climatic Change*, 75(1-2), 103-109. doi: 10.1007/s10584-005-9016-z

Fearnside, P. M. (2015, 2015/06/01/). Emissions from tropical hydropower and the IPCC. *Environmental Science & Policy*, 50, 225-239. doi: <https://doi.org/10.1016/j.envsci.2015.03.002>

Fearnside, P. M. et Pueyo, S. (2012, 06//print). Greenhouse-gas emissions from tropical dams. *Nature Clim. Change*, 2(6), 382-384.

Flanagan, L. B. et Syed, K. H. (2011). Stimulation of both photosynthesis and respiration in response to warmer and drier conditions in a boreal peatland ecosystem. *Global Change Biology*, 17(7), 2271-2287.

Giles, J. (2006, 11/30/print). Methane quashes green credentials of hydropower. *Nature*, 444(7119), 524-525.

- Guérin, F. et Abril, G. (2007). Significance of pelagic aerobic methane oxidation in the methane and carbon budget of a tropical reservoir. *Journal of Geophysical Research: Biogeosciences*, 112(G3). doi: doi:10.1029/2006JG000393
- Guerin, F., Abril, G., Richard, S., Burban, B., Reynouard, C., Seyler, P. et Delmas, R. (2006, Nov). Methane and carbon dioxide emissions from tropical reservoirs: Significance of downstream rivers. *Geophysical Research Letters*, 33(21). doi: 10.1029/2006gl027929
- Hoffert, M. I., Caldeira, K., Jain, A. K., Haites, E. F., Harvey, L. D., Potter, S. D., . . . Wigley, T. M. (1998). Energy implications of future stabilization of atmospheric CO₂ content. *Nature*, 395(6705), 881.
- Huttunen, J. T., Väisänen, T. S., Hellsten, S. K., Heikkinen, M., Nykänen, H., Jungner, H., . . . Nenonen, O. S. (2002). Fluxes of CH₄, CO₂, and N₂O in hydroelectric reservoirs Lokka and Porttipahta in the northern boreal zone in Finland. *Global Biogeochemical Cycles*, 16(1).
- Hydro-Quebec. (2018). Annual report. <http://www.hydroquebec.com/data/documents-donnees/pdf/annual-report.pdf>.
- Hydro-Québec. (2008). Romaine Environmental Impact report. *Hydro-Québec Production*.
- ICOLD. (2016). International commission on large dams. http://www.icold-cigb.net/GB/Dams/role_of_dams.asp.
- IPCC. (2007). IPCC Climate Change *Synthesis Report* (eds Pachauri, R. K. & Reisinger, A.)
- Karlsson, J., Giesler, R., Persson, J. et Lundin, E. (2013). High emission of carbon dioxide and methane during ice thaw in high latitude lakes. *Geophysical research letters*, 40(6), 1123-1127.
- Kemenes, A., Forsberg, B. R. et Melack, J. M. (2007, Jun 23). Methane release below a tropical hydroelectric dam. *Geophysical Research Letters*, 34(12). doi: Artn L12809 Doi 10.1029/2007gl029479

- Kling, G. W., Kipphut, G. W. et Miller, M. C. (1991). Arctic Lakes and Streams as Gas Conduits to the Atmosphere: Implications for Tundra Carbon Budgets. *Science*, 251(4991), 298. doi: 10.1126/science.251.4991.298
- Lehner, B., Liermann, C. R., Revenga, C., Vorosmarty, C., Fekete, B., Crouzet, P., . . . Wissler, D. (2011, Nov). High-resolution mapping of the world's reservoirs and dams for sustainable river-flow management. *Frontiers in Ecology and the Environment*, 9(9), 494-502. doi: Doi 10.1890/100125
- Lewis Jr, W. (2010). Biogeochemistry of tropical lakes. *Internationale Vereinigung für theoretische und angewandte Limnologie: Verhandlungen*, 30(10), 1595-1603.
- Lima, I. B. T. (2005). Biogeochemical distinction of methane releases from two Amazon hydroreservoirs. *Chemosphere*, 59(11), 1697-1702.
- Liu, L., Yang, Z., Delwiche, K., Long, L., Liu, J., Liu, D., . . . Lorke, A. (2020). Spatial and temporal variability of methane emissions from cascading reservoirs in the Upper Mekong River. *Water Research*, 186, 116319.
- Loken, L. C., Crawford, J. T., Schramm, P. J., Stadler, P., Desai, A. R. et Stanley, E. H. (2019). Large spatial and temporal variability of carbon dioxide and methane in a eutrophic lake. *Journal of Geophysical Research: Biogeosciences*, 124(7), 2248-2266.
- Maeck, A., DelSontro, T., McGinnis, D. F., Fischer, H., Flury, S., Schmidt, M., . . . Lorke, A. (2013). Sediment trapping by dams creates methane emission hot spots. *Environmental science & technology*, 47(15), 8130-8137.
- Mendonça, R., Barros, N., Vidal, L., Pacheco, F., Kosten, S. et Roland, F. (2012). Greenhouse Gas Emissions from Hydroelectric Reservoirs: What Knowledge Do We Have and What is Lacking? Dans.
- Mendonça, R., Müller, R. A., Clow, D., Verpoorter, C., Raymond, P., Tranvik, L. J. et Sobek, S. (2017, 2017/11/22). Organic carbon burial in global lakes and reservoirs. *Nature Communications*, 8(1), 1694. doi: 10.1038/s41467-017-01789-6

- Morales - Pineda, M., Cózar, A., Laiz, I., Úbeda, B. et Gálvez, J. Á. (2014). Daily, biweekly, and seasonal temporal scales of pCO₂ variability in two stratified Mediterranean reservoirs. *Journal of Geophysical Research: Biogeosciences*, 119(4), 509-520.
- NRC, N. R. C. (2013). Canada – A Global Leader in Renewable Energy - Enhancing Collaboration on Renewable Energy Technologies https://www.nrcan.gc.ca/sites/www.nrcan.gc.ca/files/www/pdf/publications/e mmc/renewable_energy_e.pdf, Government of Canada.
- Okuku, E. O., Bouillon, S., Tole, M. et Borges, A. V. (2019). Diffusive emissions of methane and nitrous oxide from a cascade of tropical hydropower reservoirs in Kenya. *Lakes & Reservoirs: Research & Management*, 24(2), 127-135.
- Pacheco, F. S., Soares, M. C. S., Assireu, A. T., Curtarelli, M. P., Roland, F., Abril, G., . . . Ometto, J. P. (2015). The effects of river inflow and retention time on the spatial heterogeneity of chlorophyll and water-air CO₂ fluxes in a tropical hydropower reservoir. *Biogeosciences*, 12(1), 147-162.
- Paranaíba, J. R., Barros, N., Mendonça, R., Linkhorst, A., Isidorova, A., Roland, F., . . . Sobek, S. (2018, 2018/01/16). Spatially Resolved Measurements of CO₂ and CH₄ Concentration and Gas-Exchange Velocity Highly Influence Carbon-Emission Estimates of Reservoirs. *Environmental Science & Technology*, 52(2), 607-615. doi: 10.1021/acs.est.7b05138
- Prairie, Y. T., Alm, J., Beaulieu, J., Barros, N., Battin, T., Cole, J., . . . Vachon, D. (2018, 2018/08/01). Greenhouse Gas Emissions from Freshwater Reservoirs: What Does the Atmosphere See? *Ecosystems*, 21(5), 1058-1071. doi: 10.1007/s10021-017-0198-9
- Raymond, P. A., Hartmann, J., Lauerwald, R., Sobek, S., McDonald, C., Hoover, M., . . . Guth, P. (2013, Nov 21). Global carbon dioxide emissions from inland waters. *Nature*, 503(7476), 355-359. doi: 10.1038/nature12760
- Rivkin, R. B. et Legendre, L. (2001). Biogenic carbon cycling in the upper ocean: effects of microbial respiration. *Science*, 291(5512), 2398-2400.
- Roland, F., Vidal, L. O., Pacheco, F. S., Barros, N. O., Assireu, A., Ometto, J. P. H. B., . . . Cole, J. J. (2010, Jun). Variability of carbon dioxide flux from tropical

- (Cerrado) hydroelectric reservoirs. *Aquatic Sciences*, 72(3), 283-293. doi: DOI 10.1007/s00027-010-0140-0
- Rosa, L. P., dos Santos, M. A., Matvienko, B., dos Santos, E. O. et Sikar, E. (2004, Sep). Greenhouse gas emissions from hydroelectric reservoirs in tropical regions. *Climatic Change*, 66(1-2), 9-21. doi: 10.1023/B:CLIM.0000043158.52222.ee
- Rosa, L. P., Dos Santos, M. A., Matvienko, B., Sikar, E. et Dos Santos, E. O. (2006, Mar). Scientific errors in the Fearnside comments on greenhouse gas emissions (GHG) from hydroelectric dams and response to his political claiming. *Climatic Change*, 75(1-2), 91-102. doi: 10.1007/s10584-005-9046-6
- Rudd, J. W. M., Hecky, R.E., Harris, R., & Kelly, C.A. . (1993). Are hydroelectric reservoirs significant sources of greenhouse gases. *Ambio*, 22(4), 246-248.
- Sand-Jensen, K., Pedersen, N. L. et Sondergaard, M. (2007, Dec). Bacterial metabolism in small temperate streams under contemporary and future climates. *Freshwater Biology*, 52(12), 2340-2353. doi: DOI 10.1111/j.1365-2427.2007.01852.x
- Shi, W., Chen, Q., Yi, Q., Yu, J., Ji, Y., Hu, L. et Chen, Y. (2017). Carbon emission from cascade reservoirs: Spatial heterogeneity and mechanisms. *Environmental Science & Technology*, 51(21), 12175-12181.
- Sobek, S., DelSontro, T., Wongfun, N. et Wehrli, B. (2012, Jan 4). Extreme organic carbon burial fuels intense methane bubbling in a temperate reservoir. *Geophysical Research Letters*, 39. doi: L01401 10.1029/2011gl050144
- Sobek, S., Durisch-Kaiser, E., Zurbrügg, R., Wongfun, N., Wessels, M., Pasche, N. et Wehrli, B. (2009). Organic carbon burial efficiency in lake sediments controlled by oxygen exposure time and sediment source. *Limnology and Oceanography*, 54(6), 2243-2254.
- Sobek, S., Tranvik, L. J. et Cole, J. J. (2005). Temperature independence of carbon dioxide supersaturation in global lakes. *Global Biogeochemical Cycles*, 19(2).
- Soren M., B., Paul A., d. G., Cristian R., T. et Yves T., P. (2012). Landscape heterogeneity influences carbon dioxide production in a young boreal

reservoir. *Canadian Journal of Fisheries and Aquatic Sciences*, 69(3), 447-456. doi: 10.1139/f2011-174

- Soumis, N., Lucotte, M., Larose, C., Veillette, F. et Canuel, R. (2007, November 01). Photomineralization in a boreal hydroelectric reservoir: a comparison with natural aquatic ecosystems. *Biogeochemistry*, 86(2), 123-135. doi: 10.1007/s10533-007-9141-z
- St Louis, V. L., Kelly, C. A., Duchemin, E., Rudd, J. W. M. et Rosenberg, D. M. (2000, Sep). Reservoir surfaces as sources of greenhouse gases to the atmosphere: A global estimate. *Bioscience*, 50(9), 766-775. doi: Doi 10.1641/0006-3568(2000)050[0766:Rsasog]2.0.Co;2
- Straskraba, M. et Tundisi, J. G. (1999). *Reservoir water quality management* International Lake Environment Committee Kusatsu.
- Team, R. C. (2018). R: A language and environment for statistical computing.[Google Scholar].
- Teodoru, C., Bastien, J., Bonneville, M.-C., del Giorgio, P. A., Demarty, M., Garneau, M., . . . Tremblay, A. (2012). The net carbon footprint of a newly created boreal hydroelectric reservoir. *Global Biogeochemical Cycles*, 26(2). doi: https://doi.org/10.1029/2011GB004187
- Teodoru, C., Prairie, Y. et del Giorgio, P. (2011, 2011/01/01). Spatial Heterogeneity of Surface CO₂ Fluxes in a Newly Created Eastmain-1 Reservoir in Northern Quebec, Canada. *Ecosystems*, 14(1), 28-46. doi: 10.1007/s10021-010-9393-7
- Thauer, R. K., Kaster, A.-K., Seedorf, H., Buckel, W. et Hedderich, R. (2008). Methanogenic archaea: ecologically relevant differences in energy conservation. *Nature Reviews Microbiology*, 6(8), 579-591.
- Therneau, T., Atkinson, B. et Ripley, B. (2019). *rpart: Recursive Partitioning and Regression Trees. R package version 4.1–13. 2018.*
- Thornton, W. K. (1990). Perspectives on Reservoir Limnology. In: Reservoir limnology: ecological perspectives. *Jonh Wiley & Sons, Inc.* doi: 10.2307/1467768

- Tranvik, L. J., Downing, J. A., Cotner, J. B., Loiselle, S. A., Striegl, R. G., Ballatore, T. J., . . . Weyhenmeyer, G. A. (2009, Nov). Lakes and reservoirs as regulators of carbon cycling and climate. *Limnology and Oceanography*, *54*(6), 2298-2314. doi: DOI 10.4319/lo.2009.54.6_part_2.2298
- Vachon, D., Prairie, Y. T. et Cole, J. J. (2010, Jul). The relationship between near-surface turbulence and gas transfer velocity in freshwater systems and its implications for floating chamber measurements of gas exchange. *Limnology and Oceanography*, *55*(4), 1723-1732. doi: DOI 10.4319/lo.2010.55.4.1723
- Venkiteswaran, J. J., Schiff, S. L., St. Louis, V. L., Matthews, C. J. D., Boudreau, N. M., Joyce, E. M., . . . Bodaly, R. A. (2013). Processes affecting greenhouse gas production in experimental boreal reservoirs. *Global Biogeochemical Cycles*, *27*(2), 567-577. doi: <https://doi.org/10.1002/gbc.20046>
- Victor, D. G. (1998, Oct). Strategies for cutting carbon. *Nature*, *395*(6705), 837-838. doi: 10.1038/27532
- Wang, F., Cao, M., Wang, B., Fu, J., Luo, W. et Ma, J. (2015, 2015/02/01/). Seasonal variation of CO₂ diffusion flux from a large subtropical reservoir in East China. *Atmospheric Environment*, *103*, 129-137. doi: <https://doi.org/10.1016/j.atmosenv.2014.12.042>
- Wang, F., Wang, B., Liu, C.-Q., Wang, Y., Guan, J., Liu, X. et Yu, Y. (2011, 2011/07/01/). Carbon dioxide emission from surface water in cascade reservoirs–river system on the Maotiao River, southwest of China. *Atmospheric Environment*, *45*(23), 3827-3834. doi: <https://doi.org/10.1016/j.atmosenv.2011.04.014>
- Weiss, R. F. (1970, 8/). The solubility of nitrogen, oxygen and argon in water and seawater. *Deep Sea Research and Oceanographic Abstracts*, *17*(4), 721-735. doi: [http://dx.doi.org/10.1016/0011-7471\(70\)90037-9](http://dx.doi.org/10.1016/0011-7471(70)90037-9)
- Wiesenburg, D. A. et Guinasso, N. L. (1979, 1979/10/01). Equilibrium solubilities of methane, carbon monoxide, and hydrogen in water and sea water. *Journal of Chemical & Engineering Data*, *24*(4), 356-360. doi: 10.1021/je60083a006

- Wik, M., Varner, R. K., Anthony, K. W., MacIntyre, S. et Bastviken, D. (2016). Climate-sensitive northern lakes and ponds are critical components of methane release. *Nature Geoscience*, 9(2), 99-105.
- Yvon-Durocher, G., Allen, A. P., Bastviken, D., Conrad, R., Gudas, C., St-Pierre, A., . . . Del Giorgio, P. A. (2014). Methane fluxes show consistent temperature dependence across microbial to ecosystem scales. *Nature*, 507(7493), 488.
- Zappa, C. J., McGillis, W. R., Raymond, P. A., Edson, J. B., Hints, E. J., Zemmelen, H. J., . . . Ho, D. T. (2007, May). Environmental turbulent mixing controls on air-water gas exchange in marine and aquatic systems. *Geophysical Research Letters*, 34(10). doi: 10.1029/2006gl028790